Generation of doxycycline-inducible human induced pluripotent stem cells for production of patient-derived neurons to investigate of the role of ankyrin-G in GABAergic deficits related to bipolar disorder

Author: Clayton Kramm, University of Michigan

Sponsor and Reader: Dr. Paul Jenkins, Assistant Professor of Pharmacology and Assistant Professor of Psychiatry, Department of Pharmacology
Co-Sponsor and Reader: Dr. Sara Aton, Associate Professor, Department of Molecular, Cellular, and Developmental Biology
Reader: Dr. Eleanor J. "Josie" Clowney, Assistant Professor, Department of Molecular, Cellular, and Developmental Biology

A thesis submitted in partial fulfillment of the Degree of Bachelor of Science in Neuroscience with Honors

Abstract

The neuronal role of the scaffolding protein ankyrin-G, and specifically the 480 kDa isoform product of the *ANK3* gene, has been established in mouse models as the primary organizer of the axon-initial segment throughout development. A more recently discovered role for ankyrin-G shows that it is necessary for stabilizing $GABA_A$ receptors on the axonal and somatodendritic domains of pyramidal neurons through its interaction with the $GABA_A$ receptor-associated protein. A specific variant, *ANK3* p.W1989R, abolishes this interaction and leads to dysfunction in inhibitory signaling and loss of GABAergic synapses in mouse models. Interestingly, patients with bipolar disorder (BD) present with deficits in inhibitory signaling, and a cohort of these patients has been identified who express the *ANK3* p.W1989R variant. However, findings related to this variant in mouse models cannot be applied to human bipolar disorder patients, as the complex genetic background of BD is not conserved in mice. Instead, human induced pluripotent stem cells (hiPSCs), derived from fibroblast cells of a bipolar disorder patient expressing the *ANK3* p.W1989R variant, can be used to generate neurons *in vitro* that retain the patient genetic background. Here I demonstrate the generation of hiPSCs of BD patient and control genetic backgrounds, that are capable of doxycycline-inducible differentiation to both excitatory and inhibitory neuron populations. These will be used in future experiments to assess the necessity and sufficiency of the *ANK3* p.W1989R variant to confer deficits in GABAergic signaling and synapse formation in a human-derived BD model, providing insight into a potential molecular mechanism of bipolar disorder.

Table of Contents

Scientific Acknowledgements

Initial project plans were developed by collaborator and mentor, Ph.D candidate Kendall Dean under the mentorship of Dr. Paul Jenkins and her Ph.D thesis committee. Kendall Dean provided templates for images included on figures 1 and 3. Kendall Dean and Dr. Michael Uhler performed initial transfection of hiPSCs as described in results (data not included in figures). Cooper Stinson, fellow research assistant, performed the PCR-based mycoplasma test included in Figure 3, labeled E.

Personal Acknowledgements

I would like to sincerely thank my mentor and collaborator Kendall Dean, as well as Dr. Paul Jenkins and all other members of the Jenkins Lab for their guidance and support throughout the process of performing experiments and writing my thesis. Their ability to share their knowledge and to support my journey in research has allowed me to grow in my understanding of neuroscience and the research field more than I could have imagined.

I would like to specifically thank Kendall Dean and Dr. Paul Jenkins for their time in helping me to structure and revise my thesis throughout the writing process. Not only this, but also for helping to guide and educate me while planning and performing experiments, allowing me to generate this work.

I would also like to thank my parents for their continued encouragement and support towards my academic pursuits.

Introduction

Bipolar Disorder

Bipolar disorder is a widespread debilitating neuropsychiatric disorder, affecting the lives of individuals throughout the world. This is highlighted by a lifetime prevalence rate of 1.6% for the spectrum of bipolar disorder (BD) subtypes, as determined by a study of population surveys conducted by the World Health Organization World Mental Health Survey Initiative (Merikangas et al., 2011). This disorder is identified by characteristic symptoms including episodes of extreme fluctuation in mood and cognitive affect, between a state of excessive mood elevation, known as mania, alternating with or co-occurring with a depressive state (Grande et al., 2016). A manic state consists of elevated mood, increased motor drive, and related symptoms, which is followed by a depressive state consisting of depressed mood and loss of interest or pleasure in activities, all causing social and/or occupational impairment. Within this definition, there are two subtypes of bipolar disorder. Bipolar 2 disorder is characterized by at least one episode of hypomania, including but not necessitating a subsequent depressive episode, while bipolar 1 disorder is characterized by at least one manic episode and one depressive episode in patients (Grande et al., 2016). Not only do patients present with these troublesome episodes, but BD is also known to co-occur with significant comorbidities including DSM-IV axis 1 disorders, such as substance abuse disorders, anxiety disorders, eating disorders, and more, which put patients at risk of significantly poor outcomes (McElroy et al., 2001). Even further, among BD patients, 4-19% commit life-ending suicide while 20-60% attempt suicide within their lifetime (Dome et al., 2019). Among these considerations surrounding the disorder, another complication is the frequency of recurrence of symptoms present in diagnosed patients, and it has been identified that within one year of recovery from an episode, half of all patients will have suffered a second episode (Solomon et al., 1995).

Despite the clear severity of bipolar disorder, the development of effective treatments has been hindered by difficulty in elucidating the biological mechanism of disease, as well as in identifying therapeutic targets. Additionally, most treatments focus on the stabilization of acute symptoms of mania and depression, but treatment of these individual affective states can subsequently make the other more likely (Geddes & Miklowitz, 2013). To date, a widely used long-term treatment strategy has been lithium treatment, however, long-term use involves potential for adverse side effects and limited efficacy. For example, some known disadvantages

of lithium treatment include detriments to endocrine and renal function, a slow onset of action in acute mania, as well as nausea, thirst, tremor, and more (Dols et al., 2013; Geddes & Miklowitz, 2013). Given these challenges, and in order to develop more effective interventional strategies, the molecular basis of the disorder must be investigated to identify clinical and pharmaceutical targets of intervention.

One noteworthy characteristic of BD is that it exhibits high heritability, with a value of roughly 60% heritability, as determined by numerous population level twin and family studies (Johansson et al., 2019; Song et al., 2015). Additionally, repeated Genome-Wide Association Studies (GWAS), involving BD patient cohorts, have discovered numerous genetic loci associated with the disorder with genome-wide significance. Of these genetic markers, certain genes of biological relevance have been identified, providing targets for analysis of biological dysfunction resulting from these common genetic variants and the protein products that they encode (Mullins et al., 2021; Stahl et al., 2019). Specifically, of the associated genetic loci identified through GWAS, there was strong association with genes related to neuron-specific features as well as molecules integral to synaptic transmission. Additionally, single cell gene-expression data showed that, of those genes highly associated with bipolar disorder, many are highly expressed in cortical and hippocampal brain regions (Mullins et al., 2021). This is relevant, as neuropsychiatric disorders, including BD, have been associated with disruptions in the synchrony of neuronal networks responsible for normal cognition (Bressler & Menon, 2010).

Importantly, the disruptions in neuronal synchrony observed in neuropsychiatric disorders are often attributed to disruptions in inhibitory signaling. This is a result of functionally disrupted GABA-releasing (GABAergic) inhibitory neurons, specifically GABAergic interneurons, resulting in a loss in the crucial balance between inhibition and excitation important for all stable brain states. The diverse groups of GABAergic interneurons function primarily to synapse onto excitatory pyramidal widely-projecting cells and modulate the excitatory/inhibitory input and action of these cells, providing more synchronous activity and preventing overexcitation (Marín, 2012). Loss of GABAergic inhibitory action in the brain has been identified in postmortem brain studies of patients with neuropsychiatric disorders, including BD (Benes & Berretta, 2001; Konradi et al., 2011; Torrey et al., 2005). These findings identify potential neurological contributors to this devastating disorder, and potential targets for future therapeutics.

Proposed genetic mechanisms for bipolar disorder

As a result of the severity of bipolar disorder (BD) and the significant life impairments that patients are subjected to, much research has been dedicated to discerning the neural and molecular contributors of the disorder. Due to the established heritability of BD, much research has been done to discover associated genetic risk loci that could contribute to the disorder. The use of genome-wide association studies (GWAS) has emerged as strong mechanism to identify distinct genetic markers that show association with the phenotype of different neuropsychiatric diseases. This technique is done by gathering large sample sizes of both individuals diagnosed with the disorder of interest (cases), as well as control individuals from similar population backgrounds, and collecting data on genetic markers throughout the genome for each group. The genetic markers being analyzed are single-nucleotide polymorphisms (SNPs), which are defined as a source of genetic variation involving at least two alternative nucleotides present at a genomic location that differ in distribution between individuals in the population ("Genomewide Association Studies: History, Rationale, and Prospects for Psychiatric Disorders," 2009). The SNP frequencies in a population are subjected to statistical analysis in a comparison of cases versus controls, where SNPs that are seen to be associated to a higher degree with the expression of disease are identified (Corvin et al., 2010). These SNPs that frequently co-occur with a disease of interest are known as risk-associated SNPs, and the genome regions containing or around these SNPs are identified as risk loci (Tak & Farnham, 2015). Using this technique, a variety of different variants are often identified for each disease phenotype, and these results are confirmed by replication of these studies in different large sample populations, as well as through sharing of collected data between studies. However, because it is often a variety of SNP variants arising from different genetic loci that repeatedly show association with disease, there exists debate over the individual influence of each genetic marker and the expression of the disease. It can be thought that both the commonly associated genetic variants, as well as more rare variants that are less easily detectable among populations, contribute to producing the disease phenotype in a polygenic manner (Collins & Sullivan, 2013).

Discerning the causal genetic basis of neuropsychiatric disorders including BD is challenged by characteristics of GWAS studies making identification of rare risk loci of large effect difficult, due to statistical barriers (Craddock & Jones, 1999). Therefore, future directions in assessing genetic risk factors for bipolar disorder will expand into large-scale exome and

whole-genome sequencing to identify these rare variants (Shinozaki & Potash, 2014). Nonetheless, the general consensus resulting from genome-wide studies has been the identification of multiple variant loci repeatedly presenting in diseased populations, and these genetic risk factors are largely associated with common genetic variants of small to moderate effect size due to the polygenic nature of disease (Craddock & Jones, 1999; Harrison, 2016; Kerner, 2014; Shinozaki & Potash, 2014). Despite this characterization, investigation of these risk loci could provide valuable insight into the molecular complications that arise from their variation and could contribution to disorder etiology.

One such genetic locus that has repeatedly and independently shown strong association with cases in BD GWAS studies is the *ANK3* gene locus, which is the genetic locus of the protein ankyrin-G (Ferreira et al., 2008; Sklar et al., 2011; Stahl et al., 2019). Multiple different SNP locations spanning the *ANK3* gene have been identified to have genome-wide significance in association with the BD phenotype (Ferreira et al., 2008; Fiorentino et al., 2014; Schulze et al., 2009; Sklar et al., 2011). Given this data, the variants of the *ANK3* gene and its protein product, ankyrin-G, have been identified as potential contributing actors to the BD phenotype.

Introduction to ankyrins

To understand how variants in the gene *ANK3* may contribute to the BD phenotypes, it is important to understand the ankyrin family of proteins, as well as the established and potential roles of ankyrin-G itself, which is encoded by *ANK3*. Ankyrin proteins, in general, function as structural scaffolds that connect cellular membrane-associated proteins, such as ion channels, cell adhesion molecules, and signaling proteins, with the underlying cytoskeleton of the cell, specifically actin/beta-spectrin complexes of the cytoskeleton as well as microtubules through end-binding (EB1/EB3) proteins (Cunha & Mohler, 2009; Leterrier et al., 2011). Within these networks, structural spectrin proteins associate with cytoskeletal actin filaments, as well as with ankyrin proteins. These ankyrin proteins are associated with the membrane itself and other membrane proteins, providing stability to the membrane and its individual membrane-protein complexes (Bennett & Lorenzo, 2013). This actin/beta-spectrin complex is a key component of the cytoskeleton of a variety of cell types including erythrocytes, cardiomyocytes, neurons, and more (Cunha & Mohler, 2009). It has been identified that these proteins form a specific complex in neurons, known as the membrane-associated periodic skeleton, which has been identified

along the axon, in the nodes of Ranvier, and in the dendrites to a lesser extent (Unsain et al., 2018).

The role of ankyrin in associating with a specific spectrin isoform, beta-spectrin, was first identified in erythrocytes, where it was observed that ankyrin proteins associated with both membranous anion exchanger protein, band 3, and the underlying beta-spectrin cytoskeleton (Bennett, 1979). This role has since been observed and generalized to a variety of cell types. Further, there are three distinct genes coding for the three unique ankyrin family proteins. The three distinct ankyrin genes that have been identified in vertebrates include *ANK1*, which encodes ankyrin-R; *ANK2*, which encodes ankyrin-B; and *ANK3*, which encodes ankyrin-G.

Within the different ankyrin protein products of these genes, there are conserved structural features including an N-terminal membrane-binding domain of 24 tandem ANK repeats folded as a solenoid, two ZU5 domains and a UPA domain together, a death domain, and an unstructured C-terminal regulatory domain (Bennett & Lorenzo, 2013). Within this structure, the binding site for spectrin is found in the first ZU5 domain, and the binding site for membrane proteins is found in the ANK repeat solenoid structure (Bennett & Lorenzo, 2013). Despite these similarities, there are differences in structure between these different ankyrin proteins. These differences are found specifically in the C-terminal domain which alters the binding preferences of each ankyrin protein towards membrane proteins and spectrin proteins.

Beyond these structural variations, alternative splicing of the mRNA transcripts of these individual gene products provides additional diversity in ankyrin proteins. An example of this is an isoform of ankyrin-G, product of *ANK3,* that lacks ANK repeats altogether, losing binding to membranous proteins and instead associating with intracellular organelles (Hoock et al., 1997). Furthering the observed variation in ankyrins, both ankyrin-B and ankyrin-G genetic sequences contain a vertebrate-specific giant exon found between the UPA and death domains, and these are found specifically in neuronal populations (Bennett & Lorenzo, 2013). This giant exon, and alternative splicing of it, give rise to distinct isoforms of each gene product, such as the 440 kDa isoform of ankyrin-B, as well as 480 and 270 kDa isoforms of ankyrin-G (Bennett & Lorenzo, 2013). These different isoforms are differentially expressed in different vertebrate tissues and serve different functional roles between varying cell types. With this information, the general role of ankyrin proteins as adaptor molecules between the cell membrane and the cytoskeleton has been elucidated, but the structural diversity between different ankyrin gene products and

isoforms allows for diverse applications across organs and cell types, and the conservation of these genes confer their importance.

The first ankyrin proteins to be characterized included ankyrin-R and ankyrin-B, which were shown to be differentially expressed in diverse mammalian tissues, as well as expressed in different isoforms, as a result of alternative splicing. Ankyrin-R was discovered to be highly expressed in the erythrocytes and the brain in rats, due to alternative processing of the mRNA transcript of this gene in the ankyrin regulatory domain, that allowed for this tissue specificity (Lambert & Bennett, 1993). Ankyrin-B was discovered to contain two isoforms, including a 220 kDa and 440 kDa isoform that were both identified to have brain-specific expression, and also having resulted from alternative mRNA splicing near the 3' sequence encoding the C-terminal regulatory domain (Kunimoto et al., 1991; Otto et al., 1991). Finally, ankyrin-G, encoded by the gene *ANK3,* was discovered as three main isoforms in the brain, of molecular weights of 190 kDa, 270 kDa, and 480 kDa (Kordeli et al., 1995).

Ankyrin-G

The ability of ankyrin-G to be expressed as structurally distinct isoforms allows for diverse roles for the different isoforms in numerous tissue types. The 190 kDa isoform contains the characteristic ankyrin features, including the membrane-binding ankyrin repeats domain, the spectrin-binding ZU5 domain, UPA domain, death domain, and C-terminal regulatory domain. This isoform is expressed across multiple tissues, including brain, heart, skeletal muscle, kidney, and retina (Nelson & Jenkins, 2016). Additionally, this gene encodes 480 and 270 kDa isoforms, made possible by the presence of a vertebrate-specific 7.8 kb giant exon that is expressed only within the nervous system. This exon is unique to ankyrin-B and ankyrin-G, and it encodes a unique 40 kDa subdomain that is serine and threonine-rich (Jenkins et al., 2015). This unique subdomain of the giant exon has allowed for targeted immunochemistry to determine the tissue specific expression of these larger isoforms, and they were identified in both peripheral and central neurons, specifically localized to the nodes of Ranvier and axon initial segment (AIS) in the hippocampus, cerebellum, and cerebral cortex (Kordeli et al., 1995).

The axon initial segment and the nodes of Ranvier both have distinct roles in initiating and propagating action potentials in neurons, and therefore have highly organized and clustered submembrane domains to support a variety of membrane proteins involved in these processes.

For example, both the AIS and nodes of Ranvier support a variety of voltage-gated ion channels and cell adhesion molecules, which must be properly localized to perform critical functions of action potential propagation (Chang & Rasband, 2013). Unsurprisingly, with the characteristic role of ankyrin proteins in acting as a stabilizing intermediate between membrane associated proteins and the underlying cytoskeleton, ankyrins, and specifically ankyrin-G, were suspected to play vital roles in organizing these regions. Integral ion channels that are present at the axon initial segment include voltage-gated sodium channels, which must be recruited to and stabilized at high densities within this domain in neurons. This localizing process was thought to rely on multiple proteins coordinating with each other and with voltage-gated sodium channels. These suspected proteins included a novel isoform of spectrin localized to the AIS and nodes of Ranvier, βIV-spectrin, ankyrin-G, L1 cell-adhesion molecules (L1-CAMs), neurofascin, and NrCAM (Jenkins & Bennett, 2001). Jenkins and Bennet (2001) first tested this hypothesis in mouse Purkinje neurons and discovered that ankyrin-G and βIV-spectrin colocalized at the AIS early in development, along with $Na_V1.6$, shown by overlapping signals using immunocytochemistry with protein- and cell-type specific antibodies in cerebellar Purkinje neurons. In addition to these binding partners, other suspected complex proteins were also present at the AIS, shown by immunocytochemistry, including L1-CAMs neurofascin-186 and NrCAM. Notably, Ankyrin-G and βIV-spectrin were identified to localize to the AIS at earlier developmental time points (~P2), relative to neurofascin and NrCAM (~P9), suggesting that the ankyrin-G/βIV-spectrin complex is necessary to actively recruit complex proteins at the AIS. Subsequently, using ankyrin-G exon 1B knockout mice, these researchers showed that proper localization to the AIS of βIV spectrin, L1-CAM neurofascin-186, NrCAM, voltage-gated sodium channels, and potassium channel KCNQ2 was disrupted in the mutant mice, lacking a functional form of 480 kDa ankyrin-G. These results pointed to giant ankyrin-G being a necessary protein to organize the protein complex required for sodium channel localization at the AIS, thus implying that ankyrin-G is the organizer of this domain (Jenkins & Bennett, 2001). Further studies clarified this role for ankyrin-G 480 kDa isoform, as being necessary and sufficient for organizing these proteins at the AIS in a variety of neuronal cell types through development, as well as maintaining these structures beyond development, and loss of these domains impairs normal action potential firing ability and properties (Hedstrom et al., 2008; Jenkins et al., 2015; Zhou et al., 1998).

While the AIS and nodes of Ranvier differ in their means of membrane domain formation and organization, with the AIS utilizing intrinsic organization and the nodes of Ranvier dependent on myelinating glial influence, they have in common most proteins in their domains (Dzhashiashvili et al., 2007). These structural similarities include voltage-gated sodium and potassium channels, L1-CAMs (neurofascin-186 and NrCAM), βIV-spectrin, and ankyrin-G (Hedstrom & Rasband, 2006). In a manner similar to the AIS, loss of 480 kDa ankyrin-G at the nodes of Ranvier leads to disruptions to the localization of all of these components, most importantly voltage-gated sodium channels. This shows that ankyrin-G is a necessary scaffold for these multi-protein complexes at both the nodes as well as the AIS, despite being recruited to these domains by different mechanisms (Dzhashiashvili et al., 2007; Jenkins et al., 2015). As previously stated, 480 kDa ankyrin-G-null mice lose localization of all known binding partners to the AIS, as well as formation of the AIS itself, suggesting the role of ankyrin-G as being the intrinsic organizer in this domain. By contrast, at the nodes of Ranvier, ankyrin-G binding partner neurofascin-186 appears to have an organizational role, while not required for formation in the AIS, as shown by Dzhashiashvili et al. (2007). Here, specific knockdown of neurofascin-186 using short hairpin RNA resulted in a failure to cluster ankyrin-G and voltage-gated sodium channels, as well as NrCAM, at the nodes of Ranvier, but this intervention did not prevent clustering at the AIS. Further, a subsequent knockout of neurofascin with a transfected rescue of full-length neurofascin codons reinstated the recruitment of ankyrin-G and voltage-gated sodium channels (Dzhashiashvili et al., 2007). Extracellular signals were shown to be necessary for the localization of neurofascin-186, and therefore ankyrin-G and voltage-gated sodium channels as well, to the nodes of Ranvier by expressing neurofascin-186 constructs with deletion of extracellular domains, which subsequently failed to localize at the nodes of Ranvier but maintained localization at the AIS. Finally, specific knockdown of ankyrin-G using short hairpin RNA against membrane- and spectrin-binding domains caused an absence of voltage-gated sodium channel, neurofascin-186, NrCAM and βIV-spectrin at the nodes of Ranvier (Dzhashiashvili et al., 2007). This shows that while neurosfascin has a role in recruiting ankyrin-G and other binding partners to the nodes of Ranvier, but a functional form of ankyrin-G is still necessary to scaffold and stabilize these protein complexes. These results, in collaboration with those of Jenkins and Bennett (2001) suggest that ankyrin-G has the role of intrinsically organizing the voltage-gated sodium channel and protein complexes at the AIS, which differs

from the nodes of Ranvier where ankyrin-G appears to be recruited by neurofascin-186, but where it is still necessary for the proper formation of these complexes.

Novel role of ankyrin-G in stabilizing GABAergic synapses

Beyond the established role for giant 480 kDa ankyrin-G in stabilizing the axon initial segment and nodes of Ranvier domains, different functional deficits observed in experimental organisms lacking the 480 kDa isoform suggest further functions within neurons. First, it was shown that ankyrin-G is required for the formation of "pinceau synapses" in the cerebellum. At pinceau synapses, GABAergic inhibitory interneurons synapse onto the AIS of Purkinje neurons, where it is suspected that they regulate the excitability of these neurons. The establishment of these synapses requires a steep gradient of neurofascin-186, present along the AIS of Purkinje neurons, and this gradient requires the presence of 480 kDa ankyrin-G to develop (Ango et al., 2004). Ankyrin-G null mice lose these GABAergic synapses at the AIS, due to loss of the gradient formation, suggesting a role for ankyrin-G in synapse formation, specifically in GABAergic synapses.

Interneurons, such as those present in the cerebellum and throughout the cortex, play a critical role in forming GABAergic synapses and in inhibitory transmission in the brain, synapsing primarily onto ensembles of glutamatergic, excitatory projection cells, such as pyramidal cells in the corticolimbic regions (Tremblay et al., 2016). These GABAergic interneurons are present in a diversity of subtypes, differing in characteristics such as the target domains of their axons, their firing patterns, and intrinsic membrane properties, as well as their modulatory effects on the postsynaptic neuron. Interneurons have critical roles in the cortex including modulation of circuits, regulation of firing rates of excitatory glutamatergic cells, synchronization of cortical rhythms, and balancing excitation and inhibition to prevent excess excitation (Tremblay et al., 2016). Loss of function of GABAergic interneurons has been implicated in hyperexcitability in the brain as well as various neurophysiological disorders mediated by loss if inhibitory/excitatory balance (Marín, 2012).

The majority of these interneurons target $GABA_A$ receptors on the post-synaptic cells, which are ionotropic, ligand-gated ion channels permeable to chloride ions, resulting in hyperpolarization and inhibitory effects on the postsynaptic cell (Luscher et al., 2011). These $GABA_A$ receptors are dynamic, moving laterally on the membrane to be found at both synaptic

and extrasynaptic sites in the postsynaptic cell, as well as in other locations such as on the axon initial segment (Luscher et al., 2011). Further, these receptors are subject to regulated endocytosis and recycling pathways that can alter their cell-surface expression levels (Luscher et al., 2011). Despite this, it has been shown that the presence of $GABA_A$ receptors on the post-synaptic membrane is necessary and sufficient for the formation of functional GABAergic synapses, serving as molecular targets for presynaptic GABAergic neurons (Fuchs et al., 2013). This finding emphasizes the necessity of stabilizing $GABA_A$ receptors on the post-synaptic membrane of excitatory neurons, which are the target of inhibitory GABAergic interneurons.

While the role for ankyrin-G in stabilizing GABAergic synapses of this nature was seen in pinceau synapses of the cerebellum, the role had not been discerned elsewhere in the brain (Tseng et al., 2015). Tseng et al. (2015) were the first to investigate the role of ankyrin-G in stabilizing GABAergic synapses throughout other regions of the brain and in other cell types, beyond the established role at the AIS of Purkinje neurons. This research focused on hippocampal CA1 and cortical pyramidal neuron populations, to determine the effect of ankyrin-G on stabilizing GABAergic synapses and $GABA_A$ receptors within these subtypes. These neuronal subtypes require stabilization of theses synapses, which are formed from connections with GABAergic interneurons. These researchers first used a mouse model to show specific genetic knockout of the giant exon of 480 kDa and 270 kDa isoforms of ankyrin-G provoked loss of AIS component localization, as excepted, but also caused reduced immunolabeling of vGAT (vesicular GABA transporter), a presynaptic marker of inhibitory synapses. This reduction in GABAergic synaptic immunolabeling was present in both the cell body and AIS of CA1 hippocampal tissue sections, as well as the somatic membrane and AIS of cortical pyramidal neurons in culture. Further, genetic knockout of all ankyrin-G isoforms, not solely the giant exon, was conducted using a Cre-recombinase mediated loss of expression. This resulted in eliminated immunolabeling for $GABA_A$ receptors at somatic and proximal dendrite regions, in addition to at the AIS. This result suggested that GABAergic interneurons target these locations for inhibitory synapse formation, and that ankyrin-G plays a critical role in GABAergic synapse formation.

Next, in order to determine if ankyrin-G deletion results in functional deficits in inhibitory signaling, spontaneous inhibitory post synaptic potentials were measured in cultured hippocampal neurons from an ankyrin-G null mouse model. A reduction in frequency and

amplitude of inhibitory postsynaptic potentials was seen in neuronal populations lacking ankyrin-G. These results indicate there is change in the postsynaptic $GABA_A$ receptor distribution, and importantly a decreased in the number of $GABA_A$ receptors at the membrane in this model, and that ankyrin-G plays a critical role in mediating these processes.

Importantly, ankyrin-G was also seen to be localized in these extrasynaptic somatodendritic domains, as well as along the AIS, in mature pyramidal tissue sections and cultured hippocampal neurons (post-natal day 24, day in-vitro 21). This was not observed in younger tissues (post-natal day 7 or day in-vitro 24), where ankyrin-G was restricted to the AIS, suggesting a role in stabilizing GABAergic synapses later in development. Also, this somatodendritic localization of ankyrin-G was not observed in cerebellar Purkinje neurons, where ankyrin-G is localized to the AIS, indicating that this novel role is cell type-specific. At these somatodendritic domains, ankyrin-G colocalized with known binding partners voltage-gated sodium channels and neurofascin, but interestingly, not with beta-4 spectrin, which remained localized to the AIS. In ankyrin-G null cultured neurons, neither voltage-gated sodium channels or neurofascin were present at the somatodendritic domains, showing that ankyrin-G is necessary for the recruitment of these biding partners to this domain, but not for beta-4 spectrin recruitment. This shows that beta-4 spectrin in conjuction with ankyrin-G is not necessary for GABAergic synapse stabilization. In addition to 480 kDa ankyrin-G, containing the giant exon (exon 37), the 190 kDa ankyrin-G isoform was observed localized to the somatodendritic membrane. However, in an ankyrin-G knockout mice of all isoforms, introduction of the 190 kDa isoform of ankyrin-G could not rescue GABAergic synapse localization, while rescuing with the 480 kDa isoform was sufficient to restore GABAergic synapses (Tseng et al., 2015). This result showed that the 480 kDa isoform of ankyrin-G, and specifically the full giant-exon encoded-domain, which is not present in the 190 kDa or 270 kDa isoforms, was essential for stabilizing GABAergic synapses .

Given that the role of 480 kDa ankyrin-G had now been established in the formation and stabilization of GABAergic synaptic components in CA1 hippocampal and cortical pyramidal neurons, Tseng et al. (2015) sought to understand the membrane association and binding partners of ankyrin-G that allowed for this connection. Using deconvolutions and 3D renderings, they found that ankyrin-G localized on the somatodendritic membrane in microdomains along with binding partners voltage-gated sodium channels, neurofascin, and ß2-spectrin in cortical and

hippocampal neurons. Additionally, association of ankyrin-G with these microdomains and the plasma membrane required palmitoylation of amino acid C70, as well as the presence of the giant exon, in ankyrin-G. Next, to characterize the mechanism of binding to and stabilization of $GABA_A$ receptors, these researchers used unbiased yeast-two hybrid screens of adult brain libraries to identify two potential binding partners for both ankyrin-G and $GABA_A$ receptors, including proteins GABARAP (GABA receptor-associated protein) and GABARAP-like 1. These proteins were identified by their potential for binding of the giant-exon encoded domain, as well as their known interactions with $GABA_A$ receptors. These proteins are a part of the ubiquitin-like LC3 family, which have a role in stabilizing $GABA_A$ receptors from intracellular trafficking and autophagy, promoting cell-surface expression of these receptors. To determine if ankyrin-G interacts with GABARAP *in vivo*, a proximity ligation assay was used, which showed that the two were closely localized together (within 10-15 nm), on the somatodendritic and AIS membranes. Further, isothermal titration calorimetry (ITC) using residues of GABARAP and the exon-encoded domain of ankyrin-G showed that these residues interact with a low K_D of 20 nM, showing high binding affinity for each other. The researchers proposed that this interaction could be due to a sequence of amino acids in the giant exon-encoded domain that function as a LC3-interacting motif (LIR) which has been shown to be where LC3-family proteins interact with other molecules (Birgisdottir Å et al., 2013). A key amino acid identified as part of the LIR motif in ankyrin-G was W1989, and it was hypothesized that a mutation of this tryptophan amino acid to arginine (p.W1989R) could abolish the interaction with GABARAP. Importantly, this specific mutation was identified as a human variant in the human exome sequencing project. By generating a mutant ankyrin-G protein expressing the p.W1989R mutation, researchers identified a significant decrease in interaction with GABARAP, represented by a 200-fold increase in K_D using ITC. Expression of this p.W1989R mutant in an ankyrin-G null background failed to rescue GABAergic synapses on the somatodendritic domain. This showed that the interaction between ankyrin-G and GABARAP is essential for recruiting and stabilizing $GABA_A$ receptors on the somatodendritic and AIS domains of postsynaptic cells involved in inhibitory synapses, and this is mediated through a LC3/LIR interaction encoded by the giant exon of 480 kDa ankyrin-G.

Finally, while it was now understood that ankyrin-G played a role in the establishment of maintenance of GABAergic synapses, Tseng et al. (2015) interestingly found that ankyrin-G

localization did not overlap with that of proteins gephyrin or vGAT, which are both specific markers of inhibitory synapses themselves, when using immunolabeling techniques. Ankyrin-G did colocalize with GABARAP as well as partially colocalized with $GABA_A$ receptors, and specifically more highly with $GABA_A$ receptor α4 subunit, a subunit more commonly found at extrasynaptic sites. This showed that ankyrin-G may not play an active role in synapses, but instead with $GABA_A$ receptors at extrasynaptic sites (Kittler et al., 2000). Interestingly, the clathrin-pit mediated endocytosis of $GABA_A$ receptors from the extrasynaptic site is a technique used to modulate inhibitory synaptic transmission. Given that these researchers found no change in protein levels for synaptic components in the giant-exon knockout mouse model they hypothesized that the role of ankyrin-G could be to prevent endocytosis of $GABA_A$ from the extrasynaptic sites. They showed support for this role by showing that an inhibitor of endocytosis (dynasore) restored $GABA_A$ receptors at the plasma membrane in ankyrin-g knockout neurons, and that $GABA_A$ was found at much higher intracellular levels in ankyrin-g knockout models as compared to wildtype. Therefore, Tseng et al. established that a novel role of ankyrin-G in the somatodendritic domain is to associate with GABARAP, preventing the endocytosis of and stabilizing $GABA_A$ receptors at extrasynaptic domains, a role that can modulate the inhibitory response in cortical pyramidal and hippocampal CA1 cells.

While Tseng et al. (2015) investigated this novel role for ankyrin-G at GABAergic synapses *in vitro*, this role had yet to be investigated *in vivo*. Considering this, Nelson et al. (2020) sought to characterize the role of ankyrin-G in stabilizing GABAergic synapses *in vivo* (Nelson et al., 2020). Specifically, with knowledge that mutations such as the p.W1989R mutation could abolish the interaction between ankyrin-G and GABARAP, causing endocytosis of $GABA_A$ receptors, they sought to characterize the effects of similar loss of function of ankyrin-G at the somatodendritic domain *in vivo*. This focus on the potential consequences of loss of stabilization of GABAergic synapses *in vivo* was founded upon the previously characterized necessity of stable GABAergic synapses for interneuron function, and the knowledge that disruption in inhibitory interneuron signaling has been implicated in a variety of neuropsychiatric disorders (Benes & Berretta, 2001).

To characterize the specific interactions mediating their association, Nelson et al. (2020) resolved the 3-D crystal structure of the protein complex of ankyrin-G and GABARAP to characterize the specific interactions mediating their association. They identified two amino

acids of ankyrin-G, W1989 and F1992 that comprised the suspected LIR motif and bound hydrophobic pockets in the structure of GABARAP. They also identified a novel unique binding mode mediated by a C-terminal helix, which formed salt-bridge and hydrophobic interactions with GABARAP. Using ITC and truncated ankyrin-G proteins, they identified that the minimal region capable of interaction with GABARAP was a sequence of 26 amino acids, including W1989 in the LIR motif, and this fragment associated with much higher affinity (K_d: 2.9 nM) than previously identified LIR/LC3 interactions. Introducing the p.W1989R mutation in this fragment abolished the interaction and significantly lowered the binding affinity (K_d: 11 μM) showing that this tryptophan amino acid within the LIR motif is critical for producing high affinity binding between ankyrin-G and GABARAP.

Knowing that the p.W1989R mutation in the giant exon of ankyrin-G abolishes the interaction between ankyrin-G and GABARAP, Nelson et al. (2020) generated a mouse model expressing the p.W1989R *ANK3* mutation in a homozygous manner. Previously developed mouse models, such as those with homozygous knockout of the giant exon, or homozygous knockout of the entire ankyrin-G transcript, did not survive past postnatal day 20 or birth, respectively, and developed with altered morphology in various neuronal compartments (Jenkins et al., 2015). Unlike these previous models, this model was able to survive to adulthood, and maintained ankyrin-G-mediated organization of the AIS and nodes of Ranvier, clustering all known binding partners with proper localization. This allowed for isolation of any functional deficits to be attributed to the role of ankyrin-G in the somatodendritic domain as a result of loss of connectivity with GABARAP. To observe the density of GABAergic synapse clusters, using coronal brain sections from adult (P30-35) wild type and homozygous mutant mice, these researchers used immunolabeling techniques with an antibody for the presynaptic marker of inhibitory synapses, VGAT. They found a 50-65% significant decrease in the number of GABAergic synapse clusters on the somatodendritic domain in the mutant mice relative to wild type. Additionally, using dissociated hippocampal neurons, they found a significant decrease in $GABA_A$ receptor clustering on postsynaptic membrane in the mutant mouse relative to wild type. These results suggest that abolishing the interaction of ankyrin-G and GABARAP produces reductions in inhibitory synaptic components on both the presynaptic and post-synaptic membranes *in vivo*, in accordance with the expected result of abolishing the ankyrin-G association with GABARAP and losing stabilization of $GABA_A$ receptors.

In order to assess the electrophysiological effects of this loss of GABAergic synapse clusters, Nelson et al. (2020) performed whole cell patch clamp recordings on postsynaptic neurons from mice with the p.W1989R *ANK3* mutation. Consistent with expected results for loss of inhibitory synapses, they observed a decrease in frequency and amplitude of spontaneous inhibitory post-synaptic currents in layer II/III cortical pyramidal neurons, as well as in CA1 hippocampal neurons in mutant mice relative to wild type, and reductions in both cell type were of similar magnitude. This effect was determined to be independent of action potential firing by seeing similar results in mutant mice after administering sodium channel antagonist tetrodotoxin and observing the same decreases. Finally, this effect was deemed to be mediated exclusively by $GABA_A$ receptors in the postsynaptic membrane by applying the $GABA_A$ receptor antagonist bicuculline and seeing a loss of all spontaneous inhibitory postsynaptic currents. These results suggest that, in the forebrain, ankyrin-G interaction with GABARAP is necessary for maintaining $GABA_A$ receptors at the postsynaptic membrane, and loss of this association leads to inhibitory deficits.

To assess whether this effect was exclusive to the forebrain, Nelson et al. (2020) used analogous techniques including immunostaining for VGAT and electrophysiological postsynaptic recordings in Purkinje neurons of the cerebellum, and in thalamic neurons. They found no significant difference in VGAT-positive markers on the somatodendritic region or AIS between wild type and p.W1989R mutant mice in either region, and did not observe any change in spontaneous of miniature inhibitory post-synaptic currents. This suggests that the stabilization of $GABA_A$ receptors by ankyrin-G and GABARAP in the somatodendritic domain is specific to certain brain regions as well as cell types in the forebrain. These results demonstrate the novel, necessary role played by ankyrin-G in stabilizing $GABA_A$ receptors at GABAergic synapses onto excitatory neurons. Further, these results showed reductions in the number of these synapses when the necessary interaction with GABARAP is abolished via the p.W1989R mutation of *ANK3,* suggesting loss of inhibitory tone.

The reductions in GABAergic synapse density, seen in mouse models with this mutation, are reflective of the aforementioned postmortem brain analyses of neuropsychiatric disorder patients, including bipolar disorder patients, where there was a notable reduction in GABAergic synaptic components. In keeping with this trend, Nelson et al. (2020) highlighted a family that has been identified to express the *ANK3* p.W1989R variant across multiple generations

concurrently with bipolar disorder diagnoses. First, through whole genome and exome sequencing on around 600 patients from the Heinz C. Prechter Bipolar Research Program at the University of Michigan, they identified they identified a single bipolar disorder patient expressing the *ANK3* p.W1989R variant. Further analysis of this patient's family through nested PCR of the region surrounding *ANK3* W1989, followed by sanger sequencing, found that the patient's mother and sister were also heterozygous for the *ANK3* p.W1989R variant. Notably, the patient's mother had previously been diagnosed with bipolar type 1 disorder, and patient's sister previously diagnosed with bipolar type 2 disorder. In addition, the patient's daughter was diagnosed with major depression, and she carried the *ANK3* p.W1989R variant as well. Subsequently, the heterozygous nature of the p.W1989R variant in these patients prompted Nelson et al. to perform further analogous experiments on a new mouse model which was heterozygous for the mutation, rather than homozygous. Electrophysiological recording of layer II/III cortical neurons from this mouse model demonstrated a significant, ~50 percent, decrease in frequency, as well as around 40 percent decrease in amplitude in spontaneous inhibitory post-synaptic potential for mutant mice. Additionally, measuring miniature inhibitory post-synaptic currents, they found a significant decrease in frequency and no change in amplitude in mutants relative to wild type (Nelson et al., 2020). This showed that this mutation, even when present in the heterozygous conformation, was sufficient to produced disrupted (reduced) inhibitory signaling in mouse models and could contribute to the neuropsychiatric effects seen in bipolar disorder patients heterozygous for this mutation.

Challenges with animal model

These data appear to show a link between mutations in the *ANK3* gene and altered inhibitory GABAergic signaling in the brain. A specific mutation implicated in this altered inhibitory signaling is the *ANK3* p.W1989R mutation. These findings are further consistent with genetic studies that show *ANK3* mutations coupled with decreased GABAergic signaling in postmortem patient studies, as well as inhibitory interneuron dysfunction in patients with bipolar disorder and other neuropsychiatric disorders. However, crucial considerations remain in extrapolating the results of these animal studies to human bipolar disorder patients. Mouse models are often used in neuropsychiatric research as they share 99% genetic homology with humans, including genes for neuronal components, and they also have been shown to respond to

drugs that target a variety of pathways present in the human brain, implying similar connections and molecular machinery (Howe et al., 2018). However, one challenge associated with the use of animal models to investigate the molecular basis of neuropsychiatric disorders, such as bipolar disorder, is that the symptom-based criteria that define these disorders is subjectively based in the human course of experience. Due to the complexity and polygenic nature of neurological function and its disruptions that lead to disorders, there is a lack of objective molecular or neurobiological measures to define the disease state in animals and humans. Additionally, even the existing symptom-based criteria that exist to define the disease remains subjective and vague, making it difficult to differentiate disease-states from normal mood abnormalities in humans, and especially within animal models (Nestler & Hyman, 2010).

For bipolar disorder, specifically, the cyclic nature of the disease between contrasting affective states of mania and depression has proven impossible to recapitulate in animal models, making it impossible to diagnose this disorder within animal models and establish causation through molecular mechanisms (Machado-Vieira et al., 2004). Instead, acute mood changes and disruptions are inferred in animals through observing behaviors that may serve as a reflection of the internal mood state. For example, both hyperactivity and insomnia have been proposed as behavioral states in animal models reflective of mania as experienced by bipolar disorder patients. Though these acute symptoms may resemble the human experience, they must also hold up to other measure of validity, which many fail to do. These include construct validity, which requires that the disordered is triggered in animals by similar stimuli or physiological/neurobiological events as in humans. Another measure includes predictive validity, requiring that the disordered behavior is alleviated in animals by treatments used for the analogous condition in humans (Machado-Vieira et al., 2004). Such criteria are difficult to validate due to the complex nature of bipolar disorder, involving many genetic risk loci and undiscovered plausible neurobiological deficits which may be differentially recapitulated in animal models. Therefore, despite the *ANK3* p.W1989R mutation being associated with molecular changes and neurobiological deficits in the mouse model, these cannot be specifically associated with bipolar disorder in human patients, although similar changes are anticipated.

Human induced pluripotent stem cells as a future direction

While the mouse model has provided valuable insights in the resulting neuronal dysfunction associated with the *ANK*3 p.W1989R variant, these results cannot be extrapolated to represent bipolar disorder as expressed in human patients. This is because mouse models do not harbor the complicated, holistic genetic background of bipolar disorder patients. However, the identification of bipolar disorder patients expressing the p.W1989R mutation of *ANK3* has opened a new avenue for exploration of the impacts of this mutation in neurons with an identical genetic background to the human patients.

This was made possible by pioneering work done by Takahashi & Yamanaka (2016) that discovered the ability to reprogram human differentiated somatic cells, specifically fibroblasts, into an undifferentiated pluripotent state. These reprogrammed undifferentiated cells derived from human fibroblast cells resemble embryonic stem cells in their ability differentiate into any cell type in the body, meaning they are pluripotent, and thereby were named induced pluripotent stem cells (iPSCs) (Takahashi & Yamanaka, 2016). Inspiration for this work was founded upon previous studies that identified that fusion of somatic cells with pluripotent stem cells, such as embryonic stem cells, could induce the expression of genes associated with pluripotency in somatic cells, essentially reversing their differentiation (Tada et al., 2001). Also, previous studies indicated ability for cell-type specific gene expression to convert the cell type of differentiated cells to that of the expressed genes (transdifferentiation) (Kulessa et al., 1995; Xie et al., 2004). Given this, Takahashi & Yamanaka (2016) hypothesized that expression of pluripotent cell-type-specific genes through induction of specific transcription factor expression in somatic cells could induce pluripotency. This reprogramming technique was successful in inducing pluripotency in fibroblasts of both mice and humans, and the pluripotency-associated genetic factors identified, whose forced expression was necessary and sufficient for this process, included transcription factors OCT3/4, SOX2, KLF4, and MYC (OKSM) (Takahashi & Yamanaka, 2016). Induced pluripotent stem cells, derived from fibroblast cells using this method, importantly maintain the full genetic background of the organism from which they were derived, allowing for human-specific variants to be expressed in these pluripotent cells.

The utility of these cells involves their ability to differentiate into any cell type from their induced pluripotent state, which inclined further research into the development of functional excitatory and inhibitory neuronal populations *in vitro* from these iPSCs. Generation of these

functional neuronal cultures would allow for the analysis of neuronal specific components within the genetic backgrounds of the patients from which they were derived, an important step in noticing deficits conferred by human neuronal-specific mutations. Initial attempts to generate functional neurons from iPSCs showed deficits in the efficiency of induction, the impracticality of components necessary for induction, and the differential results in achieving specific neuronal subtypes through induction (Zhang et al., 2013). However, novel methods have been developed that allow for rapid, single-step induction of functional and sub-type specific neuronal cell cultures from fibroblast-derived iPSCs through forced expression of neuronal-specific transcription factors of excitatory and inhibitory neurons, individually.

A technique for efficient induction of excitatory neuronal populations derived from hiPSCs, through specific forced transcription factor expression, was developed by Zhang et al (Zhang et al., 2013). This group had previously identified that concurrently expressing transcription factors *Brn2, Ascl1, and MytL1* successfully induced neurons from human pluripotent stem cells, but this yielded neuronal populations with variable functionality, and they were not able to identify the optimal or necessary transcription factor, for this process. To narrow the necessary transcription factor requirement, this group first expressed single transcription factors and assessed differentiation efficiency and success. They used a lentiviral infection in hESCs and hiPSCs which included a transcript for constitutive reverse tetracycline-controlled transactivator (rtTA) expression, as well as a separate infection transcript with a tetracycline-inducible transcription factor and green fluorescent marker protein (GFP) under the tetracycline-on (tetO) promoter. These described transcripts are a part of the “Tet-On” system in eukaryotic cells, where the developed rtTA protein is expressed, and binds doxycycline when it is present, causing rtTA to bind the tetO promoter and drive the expression genes downstream. This technique allows for temporal control of gene expression under the control of the tetO promoter by exogenous doxycycline application (Das et al., 2016). The results of single factor expression revealed that both *neurogenin-2 (Ngn2)* and *NeuroD1* transcription factors generated similar rapid induction of neurons, so these researchers decided to focus on neurogenin-2 as the potential sufficient factor. After plating hiPSCs and hESCS (day -2), infecting with a lentivirus transcript containing *Ngn2*, puromycin resistance, and GFP (day -1), inducing expression via doxycycline (day 0), and beginning puromycin selection (day 1), they added mouse glia to aid synapse formation (day 2) and observed differentiation. This forced *Ngn2* expression in both hESCs and

hiPSCs yielded neuron-like cells in less than one-week, and neurons that looked mature in less than two weeks, much faster than previous induction techniques. Immunostaining for stem cell-specific markers *Sox2*, *Oct4*, and *Nanog*, revealed that these were abolished in GFP-positive (virally induced) induced neurons at 21 days after transfection, indicating differentiation from their previous form. Additionally at this time point, RT-qPCR analysis showed significant increases in neuronal-specific transcripts *NeuN*, *MAP2*, and *Ngn2*. The most significant increase in expression observed was for excitatory cortical neuron-specific transcription factors *Brn2* and *FoxG1*, indicating that this induction protocol specifically generated excitatory neuronal populations. Additionally, neuronal precursor cell (NPC) markers *nestin* and *Sox2* were assessed at different time points through immunoblotting and RT-qPCR. Immunoblotting results showed that these were only expressed in the hESCs and hiPSCS and were not observed in induced neurons after 3 weeks. Through RT-qPCR, it was seen that these NPC indicators briefly increased expression shortly after viral induction, but steadily declined in expression following, indicating the switch from stem cell to neuronal-specific gene expression. Finally, the yield of these neurons was calculated, and of the surviving lentivirus-infected cells 100% of them had been differentiated to neurons, revealing that this induction technique had much more efficiency than previously used protocols (Zhang et al., 2013). All of these results indicate that expression of the single transcription factor *Ngn2* in hESCs and hIPSCs is successful and efficient in inducing cortical-like excitatory neuronal populations.

Next, to characterize the neuronal cell types produced by forced *Ngn2* expression, Zhang et al. (2013) conducted quantitative gene expression analysis on single cells using fluidigm-dependent mRNA measurements. This led to consistent gene expression profiles seen across induced neurons derived from hESCs and two different populations of hiPSCs. These expressed genes included markers characteristic of layer 2/3 excitatory cortical neurons, including *Brn-2, Cux-1*, and *FoxG1*, as well as excitatory cell-specific marker *vGlut1/2*. Additionally, these induced neurons expressed AMPA glutamate receptors GluA1, GluA2, and GluA4, but not NMDA glutamate receptors. These neurons expressed $GABA_A$ receptors, making them susceptible to inhibitory input and modulation, but lacked inhibitory neuron-specific markers vGAT and GAD, showing that they were not inhibitory neurons. Finally, these neurons lacked expression of glial and stem cell specific markers, demonstrating their differentiation and maturation into neurons. These gene expression patterns were reproduced consistently across two

lines of induced neurons from hiPSCs and one from hESCs, demonstrating the reliability of this *Ngn2*-dependent induction technique to produce mature excitatory cortical-like neurons.

Finally, the ability of these *Ngn2*-dependent induced neurons to form synapses and demonstrate functional electrophysiological activity was assessed by Zhang et al (2013). The process of synapse formation was aided by co-culturing these induced neurons with mouse glial cells. Assessments for electrophysiological activity revealed consistent ability for action potential generation, dependent on voltage-gated sodium and potassium channel currents, which were also observed. Also, repeated spontaneous excitatory post-synaptic currents (EPSCs) were observed in these cells, and were extinguishable by AMPA-receptor antagonist CNQX, consistent with observed gene expression for AMPA-type glutamate receptors. Extracellular stimulation also evoked EPSCs of large amplitude, a characteristic response of postsynaptic cells receiving robust input through multiple synaptic connections, demonstrating that those synaptic connections were present among these induced neurons. These currents were primarily AMPA-receptor mediated, but after three weeks small NMDA receptor dependent currents were observed. Importantly, the formation of electrophysiologically active synapses was observed across induced neurons derived from two different hiPSC cultures and a hESC culture, and the frequency and amplitude of spontaneous and evoked EPSCs were consistent across these. No inhibitory, hyperpolarizing currents were initially observed in these homogenous excitatory cultures, but inhibitory currents were observed following co-culturing with mouse cortical neurons. This reflects the ability of these excitatory neurons to receive inhibitory input and integrate into functional neuronal networks.

Similarly, research by Alfred et al. (2016)identified the factors necessary for optimized induction of functional forebrain inhibitory GABAergic neuronal populations derived from iPSCs (Alfred et al., 2016). First, these researchers focused on four transcription factors known to be highly expressed during GABAergic neurogenesis for cortical interneurons, including *ASCL1, DLX2, NKX2.1, and LHX6.* Next, they generated lentiviral vectors to express these different factors in human embryonic stem cells (hESCs, functionally analogous to iPSCs). To assess differentiation, they stained at day 10 following viral induction for pan-neuronal marker MAP2 and found that only *ASCL1* yielded MAP2 positive cells, specifically in 11.3% of the initial hESCs, confirmed by similar results through staining for neuronal marker βIII-tubulin. Additionally, testing expression of the three non-*ASCL1* factors in different combinations still

failed to yield neuron-specific staining, showing that *ASCL1* is necessary for differentiation. Further results from previous studies identified a phosphomutant form of *ASCL1* that was a more effective factor in neural induction, and, subsequently, expression of this mutant form (A^{SA}) in hESCs resulted in 2-fold increase in MAP-2 positive neurons relative to wildtype *ASCL1*. Using this newly identified A^{SA} in combination with the other identified factors resulted in an optimized expression pattern using A^{SA} in combination with *DLX2* and *LHX6.* This expression pattern dramatically increased the conversion of hESCs to GABAergic neurons, specifically, shown by increase in GABA and MAP2 positive cells, now 69.1% of the initial hESC population. Finally, a specific micro-RNA subtype (miR-9/9*-124) had been shown to increase neural differentiation, and coexpression of this with these optimized transcription factors significantly increased the number of MAP2-positive cells while maintaining the $GABA^+/MAP2^+$ ratio. Therefore, they identified the optimal expression pattern of A^{SA}, *DLX2,* and *LHX6* in combination with miR-9/9*-124 in hESCs to yield GABAergic-specific neuronal populations *in vitro*.

Analysis of mRNA expression in these induced neurons revealed expression of GABAergic neuronal genes *VGAT*, *GAD1*, and *GAD2*, characteristic of mature inhibitory neurons, by 35 days post-infection. These mature cells also lost all expression of genetic markers of pluripotency (*OCT4* and *NANOG*) by 48-52 days post-infection, wherein expression of cortical GABAergic interneuron-specific markers was robust, including expression of synaptic markers, AMPA and NDMA receptors, and genes responsible specifically for cortical interneuron function (*SCN1A*, *ERBB4*, *SATB1*, *ZEB2*, and *SOX6*). Immunostaining of these cells further showed expression of mature neuronal marker NeuN, axonal marker SMI-312, AIS marker ankyrin-G, and inhibitory-specific marker GAD1. Further, staining revealed localization of GABAergic synapses through overlap of gephyrin and vGAT positive puncta within dendrites (Alfred et al., 2016). These expression profiles following differentiation demonstrated the loss of pluripotency and the generation of specific mature GABAergic neurons, with characteristics of cortical interneurons.

The electrophysiological function of these neurons was assessed through patch-clamp recordings at 42 and 56 days post-infection by Alfred et al. (2016). These neurons showed fast inactivating inward and outward currents in response to voltage changes in voltage clamp recordings. Next through current injection, these neurons demonstrated action potential firing, indicating functional GABAergic membrane properties including voltage-gated sodium and

potassium channels. Importantly, when co-cultured with induced excitatory neurons, optogenetic photostimulation of GABAergic neurons elicited post-synaptic responses in excitatory neurons, which could be abolished by $GABA_A$ receptor antagonist bicuculline. This showed that activation of these induced GABAergic neurons induced an inhibitory post-synaptic response in connections with excitatory neurons, indicative of GABA release at the synapse. Finally, in assessing the post-synaptic characteristics of the induced GABAergic neurons themselves, it was noted that exogenous GABA application triggered inhibitory post-synaptic currents within the inhibitory neurons, meaning they express GABA receptors. Additionally, at 42-56 days post-infection, these neurons generated spontaneous inhibitory post-synaptic currents, indicating spontaneous quantal GABA release and connections between these inhibitory neurons. All of these results indicate that expression of specific transcription factors, dependent specifically on *ASCL1* phospho mutant A^{SA}, in hESCs can induce differentiation into functionally capable GABAergic neurons representative of mature cortical GABAergic interneurons.

Summary and experimental plans

The devastating nature of bipolar disorder, corroborated by its widespread population prevalence and its established heritability, make this disorder a critical target for discerning its physiological basis and developing effective, targeted medical interventions. While it is understood that this disorder presents a challenging polygenetic basis, the use of GWAS studies have uncovered genetic loci of interest that may have causal roles in generating the disease state in individuals. One of the most widely associated genetic locus with this disease is *ANK3*, the genetic precursor of the protein ankyrin-G. This protein, and specifically its nervous-system-specific isoforms, are understood to play several key roles in organizing functional sub-domains of neurons in the brain.

The most recently discovered role of ankyrin-G may highlight its association with bipolar disorder. At GABAergic synapses, ankyrin G associates with $GABA_A$ receptors via GABA type A receptor-associated protein (GABARAP) in somatodendritic domains in order to stabilize cell-surface expression of $GABA_A$ receptors and prevent their endocytosis. This is a necessary role for stabilizing GABAergic synapses in the brain which are generated largely by GABAergic interneurons. Loss of this function of ankyrin-G could possibly lead to inhibitory deficits and a loss of balance between excitation and inhibition. Importantly, a loss of GABAergic components

and inhibitory tone, leading to overexcitation in the brain, is a key feature discovered in post-mortem brain studies of neuropsychiatric disorder patients, including those with bipolar disorder.

While loss of ankyrin-G function has been shown to cause loss of GABAergic synapses in mouse models, this has not been studied in a human model. Thanks to the Heinz C. Prechter Bipolar Research Program, a family of bipolar disorder patients have been identified, and certain members of this family with bipolar disorder express the *ANK3* p.W1989R mutation. To assess if the *ANK3* p.W1989R mutation leads to functional deficits in inhibitory signaling in a human model, hiPSCs that maintain the patient genetic background can be used to generate functional neuronal cell cultures. In addition to neurons derived from hiPSCs with the exact patient genetic background, including the *ANK3* p.W1989R mutation, it is also necessary to generate neuronal cultures from various control genetic backgrounds in hiPSCs, allowing any potential observed deficits to be attributed to *ANK3* p.W1989R, specifically. These include an isogenic control with CRISPR-corrected *ANK3* variant, an age- and sex-matched neurotypical control, and an *ANK3* variant CRISPR knock-in age- and sex-matched neurotypical control. Patient fibroblasts are made available through our association with the Heinz C. Prechter Bipolar Research Program. These patient fibroblasts were used for reprogramming into hiPSCs and will be subjected to genetic editing to produce controls by The Human Stem Cell and Gene Editing Core at the University of Michigan.

The use of this hiPSC-derived neuron model to assess deficits conferred by the *ANK3* p.W1989R mutation has several key benefits relative to the use of a mouse model. First, the induced neurons of both the excitatory and inhibitory classes exhibit the characteristics of mature cortical-like neurons, which is the same class of neurons where *ANK3* variant related deficits were observed in mouse models. Highlighting this subtype allows for consistent analysis of predicted deficits based on mouse models, but within human populations. Next, the hiPSCs are derived from human patients with bipolar disorder that express the *ANK3* p.W1989R mutation, and the hiPSCs maintain the entire genetic background of the patient when differentiated into neuronal cultures. This allows for the full recapitulation of the genetic complexity of the patient with bipolar disorder, modeling the structure and function of their own neurons, which cannot be done within mouse models. Next, this model allows for the generation of control conditions, in which the extent of genetic complexity is retained while only manipulating the variant of interest. This allows the analysis of both necessity and sufficiency of the *ANK3* p.W1989R

variant in different hiPSC cell lines. For example, the generation of isogenic controls by correcting only the variant of interest using CRISPR, as well as using CRISPR insertion of the variant of interest into otherwise neurotypical control hiPSC cell lines will allow analysis of necessity and sufficiency, respectively. Finally, the hiPSC model allows for the generation of both excitatory and inhibitory neuron populations, both individually and in co-culture. This allows for the determination of whether deficits in inhibitory signaling previously seen in the *ANK3* p.W1989R mouse model are due to mutant ankyrin expression in excitatory or inhibitory neuron subtypes. These avenues made accessible by the hiPSC model provide the opportunity for discoveries that are particularly relevant to bipolar disorder in human populations.

In collaboration with Ph.D candidate Kendall Dean, and as a member of the Jenkins Lab in the University of Michigan Department of Pharmacology, I propose to generate doxycycline-inducible hiPSCs, using the nonviral piggyBac transposable system for the genetic insertion of transgenes. This will introduce transgenes into the genome of the hiPSCs which are necessary to differentiate hiPSCs into both excitatory and inhibitory neuronal cultures *in vitro.* These transgenes include the transcription factors *NGN2* or *ASCL1/DLX2*, which are necessary for generating excitatory and inhibitory neurons, respectively. These transgenes will be expressed using the tetracycline-on (rtTA-dependent) mechanism. Once these transgenes have been integrated, functional *in vitro* neuronal cell cultures will be produced through doxycycline-mediated differentiation, resulting in both homogenous excitatory and inhibitory neuronal cultures, as well as mixed excitatory and inhibitory cultures. Characterization of these cultures will be necessary to determine successful generation of neurons, including RNA purification for analysis of neuron-specific mRNA expression, as well as immunostaining for neuronal proteins. Following successful generation of neuronal cultures from each of the genetic backgrounds, we will perform a series of biochemical assays to determine if the ANK3 W1989R variant is necessary and sufficient to cause deficits in GABAergic signaling. We propose that this variant will result in deficits in GABAergic synapse formation, as well as deficits in inhibitory neuronal signaling. Furthermore, we predict that these deficits will be a result of the expression of the variant in excitatory neuron populations, due to the role that ankyrin-G plays in stabilizing the $GABA_A$ receptor on excitatory pyramidal neurons in mouse models. Deficits that may arise due to expression of the *ANK3* p.W1989R variant will be assessed using a series of biochemical assays. Expression of the predominant *ANK3* neuronal isoforms will be assessed at both the

RNA and protein level using RT-qPCR and western blot, respectively. Immunocytochemistry will then be used to assess localization of key GABAergic synaptic components. Finally, calcium imaging will be used to evaluate cultures for functional deficits in GABAergic signaling.

Materials and Methods

Cell Culture

Patient fibroblasts were obtained from the Heinz C. Prechter Bipolar Research Program of the University of Michigan, and subsequently reprogrammed to hiPSCs using episomal plasmids (Okita et al., 2011) as part of the Epi5 Kit (Invitrogen, A15960) by the O'Shea Laboratory, University of Michigan.

Plating and Maintenance of IPSCs

Reprogrammed hiPSCs were stored in liquid nitrogen in 0.5mL of freezing media (25.5 mL mTeSR-E8 (StemCell Technologies) with 4.5 mL DMSO(ThermoFisher) and 15 mL Knockout Serum Replacement (ThermoFisher)) until plating for use and maintenance. Prior to plating, 6-well plates were coated in Geltrex (ThermoFisher) diluted 1:100 in DMEM/F12 (ThermoFisher) and incubated at 37° Celsius for at least 30 minutes (maximum 48 hours). Frozen cells were thawed to 37° Celsius and suspended in mTeSR-Plus medium (StemCellTechnologies) containing 10 μM Y-27632 (Tocris). Serial dilutions were performed across 3 wells in a 6-well plate to establish cell culture in feeder-free conditions. Every 24 hours, media was aspirated and replaced with mTeSR-Plus medium (without Y-27632). Cells were assessed daily under microscope for visual sign of spontaneous differentiation. When spontaneous differentiation was identified, compromised colony regions were scraped off the plate and removed from culture via aspiration. Every 4-5 days, upon reaching 80 percent confluence, with circular colony morphology as well as the emergence of phase-bright centers within colonies, cells were split and passed. This was done by aspirating growth media, washing in PBS pH 7.4 (1X) (FisherScientific), and then replacing PBS with 1mM EDTA as described (Beers et al., 2012). After 5 to 6 minutes, cells were observed under the microscope until optimal clump dissociation was reached. For clump dissociation, the endpoint for EDTA dissociation was marked by rounder cell features and separation of colonies into smaller clumps of approximately 50-200 μm in size. When these features were achieved, EDTA was removed via aspiration. Cells

were then resuspended in 1 mL of mTeSR-Plus medium, and then added in a serial dilution to a 6-well plate.

Freezing hiPSCs

Alternatively, when cells reached 80 percent confluence in culture, they were frozen to expand stock of hiPSCs. This was done by removing culture media, washing with PBS pH 7.4 (1X), and then replacing with 1mM EDTA. Cells were observed under the microscope as described previously until optimal clump dissociation was achieved, and EDTA was removed. cells were resuspended in 1mL freezing media (25.5 mL mTeSR-E8 (StemCell Technologies) with 4.5 mL DMSO (ThermoFisher) and 15 mL Knockout Serum Replacement (ThermoFisher)). After resuspension, 0.5 mL clump dissociated cells in freezing were aliquoted in 1.2 mL cryogenic vials (Corning) and then slow-frozen in a Cryo 1ºC Freezing container (Nalgene) containing 250mL isopropanol at -80 degrees Celsius overnight. The next day, each cryovial of cells was transferred to liquid nitrogen for long-term storage.

Generation of Transgenic iNeuron Lines using Piggybac Insertion

First, hiPSCs were plated from liquid nitrogen freezing conditions into mTeSR-Plus medium and Y-27632, as previously described, in a serial dilution across 3 wells of a 6-well culture plate. After maintaining in culture for 4 days and assessing for appropriate colony morphology, the hiPSC's reached 80% confluence. At day -1, one of these wells was split and passed into 2 new wells using EDTA following the splitting/passing procedure outlined above.

The following day, day 0, mTeSR-Plus medium was removed from all wells and replaced it with TeSR-E8 medium. Following this, plasmids were prepared for transfection. All wells would receive 750 ng pCMV-PBase and 250 ng PB-CAG-PURO. Additionally, each of the two wells would be differentially transfected, one with 750 ng PB-TRE-hNGN2 and 750 ng PB-CAT-TetOn-IRES-eGFP to generate inducible glutamatergic neurons; and the other with .750 ng PB-TRE-hASCL1-IRES-DLX2 and .75µg PB-CAT-TetOn-IRES-mCherry to generate inducible GABAergic neurons. The plasmids for the two separate transfections were mixed with 100 µL of Opti-MEM (ThermoFisher), and each of these transfection mixtures was then combined with 7.5 µL Lipofectamine Stem Reagent (ThermoFisher) mixed with 100 µL of Opti-MEM. After mixing, the transfection mixtures were added to their respective wells. The following day, TeSR-

E8 medium with transfection mixtures was aspirated and replaced was replaced with 3 mL mTeSR-Plus medium in each well.

At day 2, the mTeSR-Plus medium was aspirated and replaced with 1mL of 1mM EDTA per well. After 7.5 minutes EDTA was aspirated and cells were resuspended in 1 mL of mTeSR Plus medium with Y-27632. The resuspended cells from each well were passed in a serial dilution to 10cm plates that had been coated in Geltrex as above, with 10mL mTeSR-Plus combined with 10µL Y-27632 in all plates. On day 3, mTeSR-Plus media was aspirated and replaced with 10 mL TeSR-E8 media per plate. On day 4, the TeSR-E8 media in each 10 cm plate was aspirated and replaced with TeSR-E8 media containing 850 ng/mL puromycin for antibiotic selection. On days 5 and 6, cells remained in the antibiotic-containing media for selection. After observing significant cell death, the TeSR-E8 media with puromycin was removed and replaced with mTeSR-Plus media for 7 consecutive days.

On day 14, the colonies of about 500 cells were manually picked and transferred to wells of a 24-well plate. Here, 12 colonies per transfection profile were transferred into 12 wells of separate 24-well plates, coated in Geltrex as above, and subsequently filled with 1.5 mL mTeSR-Plus media with Y-27632. These colonies were expanded and tested for capability of differentiation by treatment with doxycycline.

Differentiating Stable iNeuron hIPSC Lines

Cells were plated from liquid nitrogen storage as described above. When hiPSCs reached 80% confluence, cells were split and passed into 6 wells of a 6-well plate, that had been coated in 1 mL of Matrigel (Corning) diluted 1:60 in DMEM/F12 and incubated at 37° Celsius for four hours. At this step cells were passed using EDTA at 2 mM concentration to promote enhanced clump dissociation and single-cell morphology. Cells were resuspended in 1 mL mTeSR-Plus medium per well the 2 mL of resuspended cells were combined in a 25mL conical containing 18mL of mTeSR-Plus medium with 10µM Y-27632. The resuspended cell concentration was assessed by combining 10µL of cell suspension with 10µL Trypan Blue Stain and counted in an automated fashion (Thermo, Countess 3 FL). Then 500,000 cells were plated in each of the 6 wells of the Matrigel coated plate in 3mL of mTeSR Plus media containing 10 µM Y-27632.

At day 0, the mTeSR-Plus media was aspirated from all wells in the 6 well plate, and 3 mL of TeSR-E8 media containing 1mg/mL doxycycline was added per well. At day 1, the media

was aspirated and replaced with fresh TeSR-E8 media containing 1 mg/mL doxycycline. Also, additional 6-well plates were coated 0.11 g PEI (Sigma) polymer in 50 mL .1 M Borate Buffer (pH 8.4) and added at 1 mL per well of a new 6 well plate, then allowed to set at room temperature overnight. 24 hours later, PEI-coated plates were washed 5 times with WFI water (Corning) and let dry for 1 hr. Following 1 hour, 1mg/mL Laminin (Sigma) was diluted 1:100 in DMEM/F-12 and added at 1 mL per well of the 6-well plate before being incubated at 37° Celsius for 1 hour.

Finally, cells are single-cell split into the PEI/Laminin-coated plates for the continuation of differentiation and maturation of neurons. First, 3N Plus medium is prepared (125 mL DMEM/F-12, 125 mL Neurobasal-A(Gibco), 2 mL Penn/Strep, 1.25 mL Glutamax (ThermoFisher), 1.25 mL non-essential amino acids, 1.25 mL N2 supplement (Thermofisher), 2.5 mL B27(Gibco), 62.5 µL 10mg/mL insulin, .84 µL ß-mercaptoethanol (14.3 M) and combine 18 mL 3N medium with 18 µL 10 µM Y27632 and 9 µL 1mg/mL. Next, cells are split and passed following the protocol above using 2mM EDTA in PBS for enhanced clump dissociation and plating with single-cell morphology. Cells are then resuspended in 1mL of 3N media with doxycycline and Y27632. Resuspended cells are counted using automated cell counter as described above and plated in 6 wells of a 6-well plate at a density of 50,00 cells per well with 3 mL 3N media with doxycycline and Y27632. The following day, 3N media with doxycycline is exchanged for 3N media with doxycycline (no Y27632). The following 3 days, 1.5 mL of the 3mL 3N media with doxycycline is exchanged for fresh 3N media with doxycycline. After these three days, 3N media with doxycycline is exchanged for 3N media without doxycycline, and for all following days 1.5 mL of the 3 mL per well is exchanged for fresh 3N media without doxycycline.

Polymerase Chain Reaction for Mycoplasma Testing

Liquid-nitrogen stored hiPSCs were plated in a serial dilution across 3 wells of a 6-well plate coated in Geltrex (see above). The following day, media was aspirated and replaced with 3mL mTeSR-Plus medium without Y-27632. For three days, cells were incubated at 37° Celsius without exchanging media, until reaching 80-100% confluence. On the third day, samples were analyzed for mycoplasma contamination using the Mycoscope Mycoplasma PCR Detection Kit (Genlantis, Cat. No. MY01100) according to the manufacturer's instructions. For each well of

hiPSCs, a 100µL sample of culture media was taken for analysis. Each100µL sample was incubated at 95°C for 5 minutes and then briefly centrifuged to allow pelleting of cellular debris. The Mycoscope Mycoplasma PCR Detection Kit reaction mixture was prepared by adding 300µL of 5X primer to one tube of provided dNTP/Buffer Mixture. Subsequently, 10µL of the cell media was added to 40µL of the prepared reaction mixture, and 0.5µL of Taq Polymerase (on ice) was added. This mixture was homogenized by pipetting up and down, and then run in the T-100 Thermocycler (Bio-Rad) under provided cycling conditions along with a positive control (provided) and negative control (PCR water).

To run the resultant amplified DNA using gel electrophoresis, a 1.2% agarose gel was prepared by adding 1.2g Agarose to 100mL 1X Tris-Buffered Saline (TBST). The mixture was boiled and swirled before adding 5µL SmartGlow DNA Stain (Daigger). The amplified DNA samples were combined with 6X DNA Gel Loading Dye (FisherScientific). The gel was submerged in TBST, and 1 kb DNA ladder (GoldBio) and all samples were loaded at a volume of 8µL per lane. The gel was run at 120 V for roughly 25 minutes.

Resulting DNA gels were imaged using a GelDoc-It^2 310 Imaging System (UVP) and analyzed according to Mycoscope Mycoplasma PCR Detection Kit guidelines. The presence of a band for the cell culture sample reaction lanes at 500bp indicated a positive test while no band indicated a negative test.

Imaging

Fluorescent images were captured using the Leica DM IL LED Inverted Microscope, and all were captured at the same intensity and exposure time across all conditions. All fluorescent images were captured using 10X magnification. All differential interference contrast (DIC) hiPSC morphology images were captured using Invitrogen EVOS XL Core (ThermoFisher) using 10X, 20X, and 40X magnification.

Results

Generation of human induced pluripotent stem cells (hiPSCs) from patients

To generate hiPSCs from human patients, fibroblast samples must first be obtained from patients. Initially, both the identified bipolar disorder type 1 patient, as well as the age-and sex

matched control individual were identified, and a skin biopsy was performed by the Heinz C. Prechter Bipolar Research Program to obtain fibroblast samples (Figure 1, A1).

Next, the fibroblasts must be reprogrammed to a pluripotent state. This was done by the lab of Sue O'Shea, a member of the Heinz C. Prechter Bipolar Research program, reprogrammed these human fibroblasts into a human induced pluripotent stem cell (hiPSC) state (Figure 1, A2). This was done using episomal plasmids to force expression of reprogramming factors *Oct4*, *Sox2*, *Klf4*, *Lin28* and *L-Myc* as described by Okita et al. (Okita et al., 2011). To ensure that patient fibroblasts had been successfully reprogrammed to a pluripotent stem cell state, each line of hiPSCs was characterized at the Human Stem Cell and Gene Editing (HSCGE) Core. The HSCGE core used chromosomal SNPchip analysis to ensure genetic integrity, PCR to confirm an episomal vectors were not integrated during reprogramming, PCR for germ layer marker expression, and PCR for pluripotency marker expression. Importantly, these hiPSCs maintained the genotype of both the patient with bipolar disorder (cell line BP7G) who expressed the *ANK3 p.*W1989R variant of interest, as well as that of an age- and sex-matched control individual (cell line C8WW (Figure 1B) (BP7G henceforth referred to as patient, C8WW as control).

To obtain a sufficient stock of these hiPSC cell lines, multiple months were focused on the expansion and freezing down of these cell lines. Using the protocols listed above for plating hiPSCs from liquid nitrogen storage, maintaining with daily maintenance, splitting and passing, and finally re-freezing cells, I generated 37 cryovials of the control hiPSC cell line and 20 cryovials of the patient cell line, stored in liquid nitrogen. Throughout this process, I monitored cells in culture for adequate human embryonic stem cell-like morphology as described, highlighted by Okita et al. as round, flat colony morphology characterized by large, visible nuclei and low levels of cytoplasm (Okita et al., 2011) (Figure 1C). Only cells displaying this adequate morphology were selected to be stored in liquid nitrogen storage. Additionally, cells were monitored for spontaneous differentiation, characterized by abnormal three dimensional or rosette structures within colonies, loss of defined circular colony borders, and loss of characteristic human embryonic stem cell-like morphology. When this arose, I cleaned off spots that were abnormal in appearance by manually scraping the affected portion of the colony off the plate and aspirating the cell media. Additionally, I routinely used PCR to test for mycoplasma contamination of the hiPSC cultures that I was maintaining. Through these methods, I was able to generate a sufficient supply of stem cells of both genotypes for all future experiments.

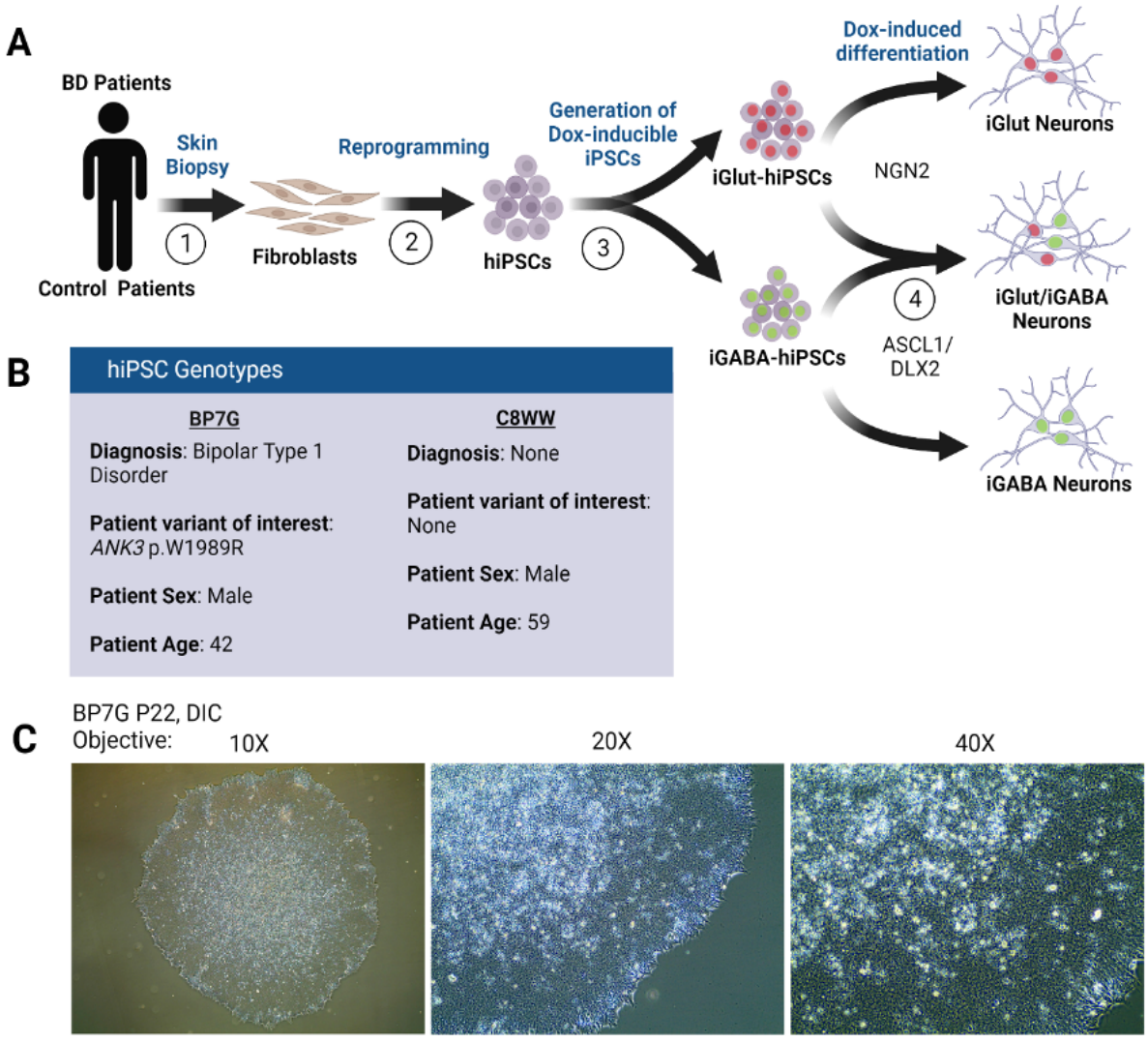

Figure 1: Overview of experimental steps and hiPSC morphology. *A) Workflow of experimental procedures in steps for generation of hiPSC-derived neurons from patient fibroblast samples. Cartoon adapted from Kendall Dean, unpublished B) Genotype and description of patients from which hiPSC cell lines were derived. C) Representative differential interference contrast (DIC) microscopy images of hiPSC line BP7G, at passage 22, displaying optimal colony morphology.*

Generation of transgenic doxycycline (Dox)-inducible hiPSCs using PiggyBac transposition

After aggregating a sufficient stock of hiPSCs with both genetic backgrounds, it was necessary to generate stable hiPSC cell lines, capable of doxycycline-inducible differentiation

into neuronal cell cultures. To generate stable hiPSC lines that express doxycycline-inducible transcription factors, allowing for subsequent differentiation into neuronal cells, one must integrate the necessary transgenes in the hiPSC genome (Figure 1, A3).

For this, we used the PiggyBac (PB) transposable technique, which is a binary transposable system in which the PiggyBac transposase enzyme can be encoded on a separate vector relative to the transgenic DNA sequence intended for transposition. This DNA for transposition into the genome is integrated into the PB sequence (2.4 kb), flanked by 13 bp terminal inverted repeat sequences target by the transposase enzyme. This cut and paste mechanism results in the integration of the transgene within the PB sequence at TTAA segments within the targeted host genome, and unlike other mammalian transposition methods leaves no unwanted DNA footprint in the sense of transposition of unwanted base pairs, as transposition is done with high efficiency relative to other methods (Zhao et al., 2016).

Using the PiggyBac transposon method, we sought to generate stable cell lines of both patient and control hiPSC genotypes, capable of doxycycline-inducible differentiation to both excitatory (glutamatergic) and inhibitory (GABAergic) neuronal populations, each. Therefore, all target cells were transfected by Kendall Dean and Dr. Michael Uhler, within the Uhler Lab at the University of Michigan, with pCMV-PBase (PiggyBac transposase) as well as a vector conferring PiggyBac mediated puromycin resistance (PB-UbC-puro) (Figure 3A,C). The remaining vectors for doxycycline-inducible expression were specific to generation of glutamatergic neurons (excitatory) or GABAergic neurons (inhibitory). For glutamatergic neurons, the vectors included PB-UbC-rtTA-IRES-eGFP and PB-TetO-hNGN2 for doxycycline-inducible expression of transcription factor *NGN2* (Figure 3A). For GABAergic neurons, the vectors included PB-UbC-rtTA-IRES-mCherry and PB-TetO-ASCL1S5A-IRES-DLX2 for inducible transcription factors *ASCL1* and *DLX2* (Figure 3C). Successful transfection was assessed by both the analysis of homogenous fluorescent protein expression patterns within individual colonies (excitatory culture populations marked with GFP, inhibitory culture populations marked with mCherry), as well as an antibiotic selection using puromycin. Following antibiotic selection, individual colonies were isolated as clones within wells of a 24-well plate, where 12 colonies per genotype were picked and isolated for both excitatory and inhibitory populations. Continual assessments were conducted for hiPSC morphology, lack of spontaneous differentiation, and homogenous fluorescent patterns. Finally, individual clones

were transferred to a 6-well plate, cultured, and treated with doxycycline to assess for differentiation capability. Successful clones were then expanded in culture, and frozen to be stored in liquid nitrogen to generate a large stock of stable doxycycline-inducible hiPSC cell lines, to generate excitatory or inhibitory neuron populations, for both control and patient genotypes.

Generating patient-derived neurons from dox-inducible hiPSCs

Once stable cell lines were established with integrated doxycycline-inducible transcription factors specific for neuronal differentiation, I began the differentiation process to generate cultures of excitatory and inhibitory neurons for both hiPSC genotypes (Figure 1, A4). I selected an individual clone (clone 5) of the patient genotype, frozen in liquid nitrogen (.5 mL) and plated these cells in a serial dilution across three wells of a 6-well plate in mTeSR-Plus medium with Y-27632. After maintenance and growth of colonies, to 80% confluence within the densest well, I split and passed cells from this well to six wells of a 6-well plate, in a 1:12 dilution with mTeSR plus with Y-27632, to establish colonies of smaller size. After 72 hours in culture, the cells were 80% confluent in smaller colonies. At this point, cells were to be split and passed with the desire of establishing single-cell culture rather than colonies, for the facilitation of doxycycline treatment and differentiation. For this, six wells of a 6-well plate were coated in Matrigel, rather than Geltrex, to facilitate differentiation, and cells were split and passed in single-cell morphology at a density of 500,00 cells per well. 24 hours later, I exchanged media to TeSR-E8 medium with doxycycline (5µg/mL) to begin the differentiation. However, 24 hours following this step, on November 24, 2022 a routine PCR-based mycoplasma test was performed on the hiPSC cell line of mentor and collaborator Kendall Dean, and this test returned positive. Upon further testing, the control line for which I had begun differentiation also tested positive for mycoplasma contamination.

Mycoplasma contamination and elimination in hiPSCs

Mycoplasma, in its various strains, comprise a large class of prokaryotic bacterial cells known as *Mollicutes,* characterized by their extremely small size relative to other prokaryotic cells (300-800 nm in diameter), slow growth yielding generation times of between one and nine hours, and lack of a rigid cell wall. Importantly, mycoplasma, and in particular the strains

Mycoplasma hyorhinis, *Mycoplasma orale*, *Mycoplasma arginini* and *Acholeplasma laidlawii,* are known as prolific contaminants of cell culture, occurring in between 5 and 35% of cultured cells (Hay et al., 1989). The contamination of a cell lines by mycoplasma has diverse effects on the host cell, depending on the strain of mycoplasma as well as the identity of the host. Many are capable of causing cytopathic effects, but this can go undiscovered as this cytopathology is often not externally visible (Rottem & Barile, 1993). The notably small genome of mycoplasma cells requires that many strains exert parasitic effects on host cells, with strains that require nucleic acid precursors, amino acids, fatty acids, and sterols, using the host cell as a source.

Additionally, certain mycoplasma strains can consume the cultured-cell growth medium, using its nutrients as an energy source and depriving the cultured cell line of critical nutrients, often consequently producing byproducts toxic to cultured cells. Among these other negative consequences of mycoplasma infections have been seen such as affected protein synthesis, membrane receptor function, signal transduction, as well as promoting chromosomal abberations and viral infections (Rottem & Barile, 1993).

Specifically in relation to hiPSCs, it has been found that infection of murine embryonic stem cells with mycoplasma strains *M. hominis, M. fermentans, and M. orale* caused reduced growth rate and viability, as well as chromosomal abberations (Markoullis et al., 2009). The most common sources of mycoplasma contamination include laboratory technicians for which various strains of mycoplasma reside in the human oropharyngeal tract, bovine serums used as reagents, and propagation from other infected reagents or cell lines used in the environment of cultured cells (Nikfarjam & Farzaneh, 2012). These contaminations additionally often go undetected, as the infection often does not result in overt cytotoxicity to cells, and the lack of cell wall and small diameter make mycoplasmas difficult to visualize (Nikfarjam & Farzaneh, 2012). Therefore, without routine tests, mycoplasma colonies can easily achieve 10^7 to 10^8 colony forming units per mL without causing visual perturbations in cell culture (Hay et al., 1989). Further, the lack of cell wall characteristic of all mycoplasma species renders them immune to commonly used antibiotics, making it difficult to restore cultures after being infected (Hay et al., 1989; Nikfarjam & Farzaneh, 2012).

Given the large range of negative effects that a mycoplasma contamination can confer towards cultured cells, this was devastating news causing the forced abandonment of the differentiation process and the beginning of subsequent testing of all other cell lines and reagents

that had been in use. Following sterilization of the tissue culture hood, all reagents and cell lines in liquid nitrogen storage were assessed for mycoplasma infection using the Mycoscope Mycoplasma PCR Detection Kit (Genlantis, Cat. No. MY01100). This kit is able to detect fewer than 5 mycoplasma genomes per microliter of sample, and its primer is specific to the highly conserved 16S rRNA coding region in the mycoplasma genome, allowing detection of all common mycoplasma species. Kendall Dean and I began by testing all reagents that had been used for any of the stem cell procedures, including maintenance, splitting and passing, freezing, transfecting, and differentiating, and plate-coating for contamination. The results of these tests indicated only reagents that had been previously opened while in the culture hood where contaminated cells were also present were contaminated, while all fresh reagent stocks were mycoplasma negative. Upon testing cell cultures, including both active cultures as well as previously frozen stocks of hiPSCs, we determined that all clones of the stable hiPSC lines that had been transfected with doxycycline-inducible factors were positive for contamination (Figure 2A,B), while the hiPSCs that been generated previously and stored without transfection tested negative (Figure 2C,D). This allowed us to deduce that the contamination originated during the time of the transfection procedure.

The laboratory the transgene integration procedure was performed in utilized an alternative mycoplasma testing procedure using qRT-PCR, which had a higher threshold of detection than the PCR-based method we had been using. When we reviewed the data from the qRT-PCR conducted in the Uhler Lab during the transgene integration, it became apparent that there were low levels of mycoplasma detected at the time of the test. However, we had missed the presence of mycoplasma contamination in weekly PCR-based detection tests that we routinely preformed while expanding the stock of the transfected stable clones. We concluded that this was because, for cell maintenance, we exchanged the cell medium daily, including on days before tests, not allowing sufficient time for mycoplasma to contamination levels to increase to a detectable level by our detection method. Therefore, at all points going forward, we decided to allow the cell medium to remain on the cells that would be subject for testing for 72 hours prior to testing to allow for sufficient mycoplasma colonization prior to testing, if it were present. Nonetheless, this contamination led to the loss of all hiPSCs with stably integrated inducible transcription factors, capable of differentiation into neurons, leaving us with the task of generating new clones of these lines both the control and patient genotype hiPSCs.

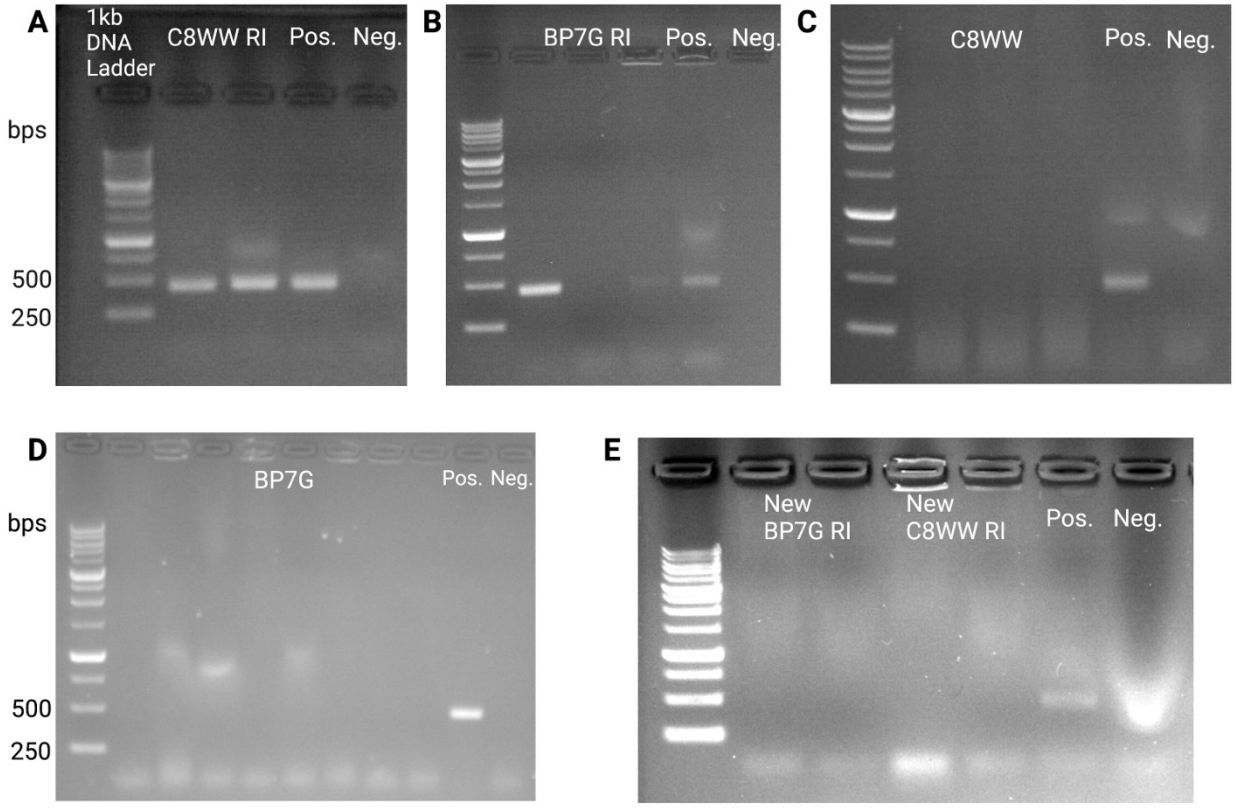

Figure 2: PCR-based mycoplasma detection assay results for various hiPSC cell lines. *Band presence at 500 base pairs on 1 kb ladder indicates mycoplasma-positive result A) Positive test result for inhibitory hiPSC stable cell line generated by Dr. Michael Uhler and Ph.D candidate Kendall Dean, genotype C8WW (12/01/2022) (RI = red inhibitory). B) Positive test result for inhibitory hiPSC stable cell line generated by Dr. Michael Uhler and Ph.D candidate Kendall Dean, genotype BP7G (01/09/23.) C) Negative test result for hiPSC genotype C8WW, obtained from Human Stem Cell and Gene Editing Core and expanded by me (02/10/23.) D) Negative test result for hiPSC genotype BP7G, obtained from Human Stem Cell and Gene Editing Core and expanded by me (02/06/2023). E) Negative test result for most recent stable inhibitory hiPSC cell clones of genotypes C8WW and BP7G, transfected by me (03/28/23).*

Generation of mycoplasma-free transgenic doxycycline (Dox)-inducible hiPSCs using PiggyBac transposition

Given that all stable hiPSC lines, of patient and control genotypes, that had successfully integrated the doxycycline-inducible transcription factors necessary to generate GABAergic (*ASCL1/DLX2)* and glutamatergic (*NGN2*) neuronal cell populations had been contaminated with mycoplasma, it became urgently necessary to generate new lines of these cells (Figure 1, A3). I began this process by selecting a cryovial of hiPSCs with the patient *ANK3* p.W1989R genotype from liquid nitrogen storage, which had been previously obtained from the Human Stem Cell and Gene Editing (HSCGE) Core at the University of Michigan. These cells were confirmed mycoplasma negative by the HSCGE core before freezing using PCR. I plated these cells in mTeSR-Plus medium with Y-27632 on a Geltrex-coated six-well well plate, in a serial dilution across three wells.

Next, I began the process of generating transgenic hiPSCs with doxycycline-inducible transcription factors for neuron generation on the densest well (80% confluent). This process began with splitting this confluent well using 1mM EDTA into two separate wells of a Geltrex-coated six-well plate containing mTeSR-Plus medium with Y-27632. The following day, I prepared the transfection DNA complexes by combining the respective DNA vectors with Opti-mem and Lipofectamine-STEM reagent. One complex contained the 750 ng PB-TRE-hASCL1-IRES-DLX2 DNA and 750 ng PB-CAT-TetOn-IRES-mCherry DNA for generation of doxycycline-inducible GABAergic neuron cultures (Figure 3C), while the other contained 750 ng PB-TRE-hNGN2 and 750 ng PB-CAT-TetOn-IRES-eGFP for generation of doxycycline-inducible glutamatergic neuron cultures (Figure 3A). Both complexes contained 750 ng pCMV-PBase and 250 ng PB-CAG-PURO, each, for constituent expression of the PiggyBac transposase enzyme and PiggyBac-transposon dependent integration of puromycin resistance, respectively (Figure 3A,C). Transfection was performed by aspirating mTeSR-Plus medium and exchanging it for TeSR-E8 medium in each of the two wells three hours before transfection, incubating to 37° Celsius, and then adding each DNA complex dropwise to its respective well three hours later. After 24 hours of incubation at 37° Celsius, the media containing the transfection complexes was removed and replaced with mTeSR-Plus, and transfection efficiency was analyzed by fluorescence microscopy, where it appeared that around 40% of the cells had been successfully transfected in each well.

Next, each well of transfected cells was split into 3, 10cm plates done using 2mM EDTA, rather than 1mM to enhance dissociation of cells, and the cells were resuspended with extensive pipetting to ensure the breakup of colonies. The cells from each well were plated at single-cell density in a serial dilution across three Geltrex-coated 10cm plates each, using mTeSR-Plus medium with Y-27632, which was exchanged for mTeSR-Plus without Y-27632 24 hours later. It was crucial that cells were plated as single cells and not as clumps of cells for this step so that each colony that would eventually form would be clones of identical genetic identity. After 48 hours, the mTeSR-Plus medium was exchanged for TeSR-E8 medium. 24 hours after this, TeSR-E8 was exchanged for TeSR-E8 medium containing .85μg/mL puromycin to perform a selection against cells that had not integrated the appropriate vectors during transfection. This repeated the next day to ensure adequate selection.

Following these two days of selection, significant cell death was observed, leaving only small colonies developing from single-cell origin that had all integrated the appropriate vectors. For the next seven days, cells were maintained in mTeSR-Plus medium, allowing for the growth of colonies with homogenous fluorescent expression patterns, originating from a single-cell state. Once colonies had grown sufficiently and established proper hiPSC colony morphology without spontaneous differentiation, I began to choose colonies with homogenous fluorescent appearance to manually pass into wells of a 24-well plate. This would allow colonies to be isolated as individual clones, from which point the clones with the most ideal morphology and homogenous fluorescence of medium-high intensity could be expanded and stored in liquid-nitrogen as stable cell lines. I performed manual passage of individual colonies by passing a p200 pipette tip across the bottom the plate region containing the colony of interest, while subsequently releasing the plunger to draw in the cells. Each colony was passed into a single-well of a 24-well plate with Geltrex coating and 1 mL of mTeSR-Plus with Y-27632 in each well. I isolated 12 colonies from the hiPSCs transfected with glutamatergic transcription factors, and 12 colonies from the hiPSCs transfected with GABAergic transcription factors. Subsequently, a mycoplasma test was performed using the media from the inhibitory-transfected hiPSCs of both genotypes, C8WW and BP7G, as representative samples of the mycoplasma contamination state of the cultures. These test results indicated that all transfected cells were mycoplasma-negative and were ready to be isolated as individual clones (Figure 2E). After allowing the reformation of colony morphology in each well through maintenance with mTeSR-Plus medium, clones with optimal

homogenous fluorescence and hiPSC colony morphology were chosen to be expanded for storage, as well as assessed for capability of differentiation (Figure 3B,D). Each isolated clone that will be used for future neuron differentiations will be individually tested for mycoplasma during expansion.

The next stage of this process will be to treat each clone with doxycycline for three days and analyze induction of transcription factor expression using qRT-PCR and determine if clones begin to take on neuronal morphology in the presence of doxycycline. The most promising clones will then undergo the full differentiation protocol and be analyzed for neuronal morphology and expression of neuronal factors indicative of excitatory and inhibitory neuronal populations (Figure 3E). Clones that display the expected characteristics will then be utilized for experimentation to test the impact of the *ANK3* p.W1989R variant on inhibitory signaling.

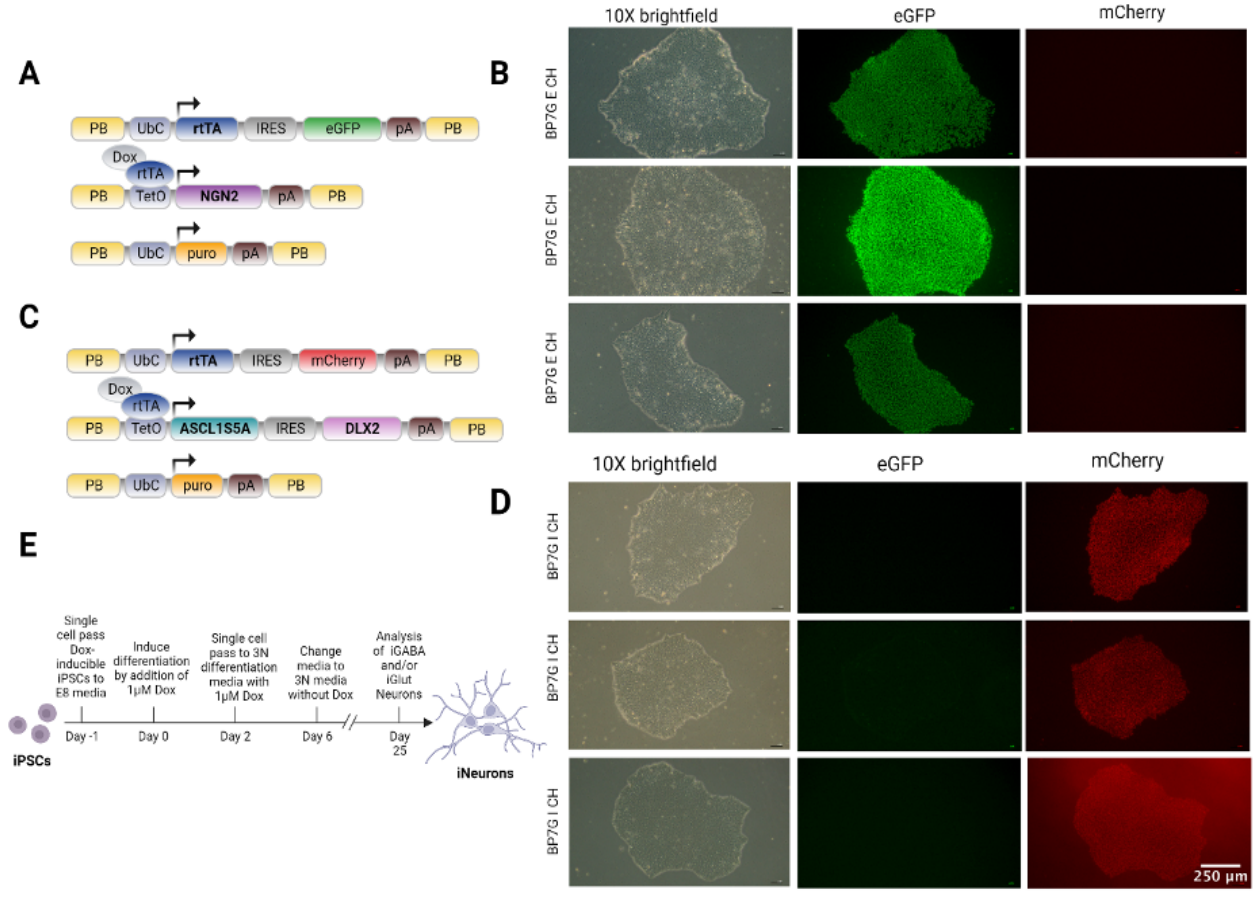

Figure 3: Genetic constructs and results for generation of mycoplasma-free transgenic doxycycline (Dox)-inducible hiPSCs using PiggyBac transposition. *A) Genetic vectors for*

PiggyBac transposition and generation of doxycycline-inducible hiPSCs of glutamatergic, excitatory character. B) 10X colony morphology and homogenous eGFP expression for generated hiPSC Clone H, BP7G genotype of excitatory character. C) Genetic vectors for PiggyBac transposition and generation of doxycycline-inducible hiPSCs of GABAergic, excitatory character. D) 10X colony morphology and homogenous mCherry expression for generated hiPSC Clone H, BP7G genotype of inhibitory character. E) Workflow for doxycycline-induction of mature iNeurons from hiPSC clones over 25 days. Cartoons in panels A, C, and E, adapted from Kendall Dean, unpublished.

Future directions

In the future, it will be critical to further this progress that has been made, specifically while vigilantly testing for contaminants such as mycoplasma. This will be done through a variety of experiments using the hiPSC-derived, mature neuronal cultures that will be generated from bipolar disorder patient and control genetic backgrounds. These experiments will have the aim of corroborating findings in mouse models, which indicate that ankyrin-G has a role of stabilizing inhibitory synapses in the forebrain, through its interaction with GABARAP, and that this interaction is abolished through the *ANK3* p.W1989R variant leading to a decrease in inhibitory synapses and disruptions in inhibitory signaling (Nelson et al., 2020; Tseng et al., 2015). We hypothesize that mixed cultures of excitatory and inhibitory hiPSC-derived neurons will show deficits in GABAergic synapse formation, observed through loss of localization of key inhibitory synaptic components in excitatory neurons. Further, we hypothesize that deficits in inhibitory synapse formation will lead to decreases in inhibitory signaling, observed using calcium-imaging experiments for network activity and synchronization in mixed cultures of excitatory and inhibitory hiPSC-derived neurons.

For these future experiments, we will generate mature cultures of excitatory and inhibitory neurons, as well as co-cultures. This will be done through 25 days of doxycycline treatment to induce hiPSC expression of the integrated, PiggyBac-inserted, transcription factors, leading to homogenous and mature cultures of GABAergic and glutamatergic neurons (Gupta et al., 2018; Wang et al., 2017; Yang et al., 2017). Throughout the differentiation process, a series of RNA purification assays will be performed to assess the progress of differentiation, using subsequent RT-qPCR analysis. Differentiation will be observed as the loss of expression of

pluripotency markers and the attainment of expression of neuron-specific mRNA transcripts. The pluripotency markers that will be assessed include *NANOG*, *OCT4*, *SOX2*, and *KLF4*, and we expect a steady decline as the differentiation progresses over the course of 25 days. The increase of expression of neuron-specific genes, indicating the successful neuronal differentiation, are also expected to be seen. For GABAergic populations, we will assess expression levels of GAT1, vGAT, $GABA_A$ receptor, and GAD1/2, and will also screen for expression of glutamatergic cell markers such as hNeurogenin, vGlut, and Snyapsin expecting to see the absence of or very low levels of their expression. For glutamatergic neuron populations, the same markers will be screened for with the opposite expected results (Wang et al., 2017; Yang et al., 2017; Zhang et al., 2013). Once characterized and differentiated into homogenous and mature neuron cultures, we will perform experiments that assess the suspected role of the *ANK3* p.W1989R variant in neurons derived from bipolar disorder patients.

First, it we will assess if the *ANK3* p.W1989R variant will lead to decreased levels of expression of *ANK3* mRNA, in its different isoforms, as well as the resulting ankyrin-G protein, relative to control neurons. Previously, it was shown, using hippocampal and cortical lysate protein expression analysis in mice expressing the *ANK3* p.W1989R variant, that there was no change in expression levels of 270 or 480 kDa ankyrin-G within variant neurons, but there was a 50% decrease in 190 kDa isoform expression (Nelson et al., 2020). Therefore, within hiPSC-derived neurons expressing the variant, we expect analogous results in expression levels of the different isoforms of ankyrin-G. If expression levels in the hiPSC-derived neurons deviated from these expected results, it could provide an alternative hypothesis to deficits seen in other parameters, such as GABAergic synaptic component localization or GABAergic signaling.

Following this, we will perform immunostaining and confocal microscopy to identify the localization of key GABAergic synaptic components in all genetic backgrounds. This experiment will be performed on the basis of findings that the interaction between ankyrin-G and GABARAP at the somatodendritic regions of excitatory neurons is necessary to oppose endocytosis of $GABA_A$ receptors and to conserve their clustering at the membrane to form functional GABAergic synapses, and this interaction is abolished with the *ANK3* p.W1989R variant (Tseng et al., 2015). One such finding, using *in vitro* ankyrin-G null mouse cortical and hippocampal neurons, showed that rescue with p.W1989R ankyrin-G was insufficient to restore GABAergic synapses on the somatodendritic and AIS membranes, identified by loss of

immunolabeling for inhibitory synaptic markers $GABA_A$ receptor ß2/3 subunits, gephyrin, and vGAT, relative to wild type ankyrin-G rescue (Tseng et al., 2015). Further, when *ANK3* p.W1989R is expressed in mouse models *in vivo*, a loss of inhibitory presynaptic marker, vGAT, is observed, as well as a significant loss of postsynaptic GABAergic synapse clusters in both cortical and hippocampal neurons (Nelson et al., 2020). This shows that the localization of both pre- and post-synaptic markers of inhibitory synapses is altered in the *ANK3* p.W1989R variant mouse model. These findings will be assessed in the human cortical-like neuron model of this variant to assess if localization of key inhibitory synaptic components is altered in the resulting phenotype, suspectedly leading to altered GABAergic function. This will be done by generating co-cultures of mature cortical-like excitatory and inhibitory neurons and immunolabeling GABAergic synaptic components with fluorescent antibodies against GABARAP, the $GABA_A$ receptor, and vGAT, followed by confocal microscopy, where we will be able to visualize the localization of these components by visual fluorescence.

Comparisons in localization of components and GABAergic synapse formation between the bipolar disorder patient line and controls will allow the determination that variant alters GABAergic synapse formation in the patient genetic background. Comparing the BD p.W1989R variant-expressing neurons with the isogenic control will allow us to test the necessity of the variant to alter the localization of key GABAergic signaling components. Next, comparing the neurotypical control neurons with the neurotypical control ANK3 p.W1989R knock-in neurons will allow us to test the necessity of the variant to alter the localization of key GABAergic signaling components. Finally, generating mixed populations of excitatory and inhibitory neurons, with the variant in only one of the neuron types, will allow us to determine if the effect of the variant is due to its expression in inhibitory, presynaptic or excitatory, postsynaptic neuron populations. In this mixed culture format, we expect the variant to be necessary and sufficient to generate these deficits, and we predict that the deficits arise from specific expression of the variant in excitatory neuron populations.

Additionally, we will characterize network activity through calcium imaging in co-cultures of excitatory and inhibitory human-derived neurons. This experiment is based on findings that the *ANK3* p.W1989R variant, expressed in mouse models, hinders GABAergic inhibitory signaling. This was first observed in cortical and hippocampal neurons *in vitro*, in which rescue with p.W1989R ankyrin-G in an ankyrin-G null mouse was insufficient to restore

both the frequency and amplitude of miniature inhibitory postsynaptic currents relative to rescue with wild-type 480 kDa ankyrin-G (Tseng et al., 2015). In addition, whole-cell patch clamp recordings of acute brain slices in homozygous p.W1989R variant mice showed reduced frequency and amplitude of spontaneous inhibitory postsynaptic currents (sIPSCs) in cortical and hippocampal neurons relative to wild type (Nelson et al., 2020).

To relate these findings to network synchronization in the brain, Nelson et al. assessed the function GABAergic parvalbumin-positive (PV+) interneurons, which act in the forebrain to promote network synchronization due to their ability to synapse onto hundred to thousands of excitatory pyramidal cells. These researchers hypothesized that decreased GABAergic synapses and sIPSC frequency in the *ANK3* p.W1989R model could be due either to a lower density of PV+ interneurons or reduced synaptic connections of these neurons. However, these researchers observed no change in the density of these PV+ neurons with immunolabeling, nor any significant changes in their firing properties using evoked action potentials, such as action potential frequency and amplitude, in the somatosensory cortex variant mice relative to wild type. These findings were corroborated in the investigation of two other classes of GABAergic interneurons within the somatosensory cortex, regular spiking non-pyramidal neurons and irregular spiking interneurons, for both of which they found no difference in action potential frequency or amplitude (firing properties) with evoked action potentials. However, all classes of interneurons showed decreased synaptic connectivity, pointing towards the conclusion that the reductions in $GABA_A$ receptor mediated inhibitory signaling in variant mice is due to decreased connectivity and therefore inhibitory synapse formation, consistent with earlier findings.

Further, based on the role of PV+ interneurons in generating network synchronization resulting in the formation of gamma oscillations, these researchers hypothesized that decreased GABAergic synaptic connections of these neurons would alter network synchronization, resulting in gamma oscillations of lower power. This result was seen in the variant mouse population within CA1and CA3 hippocampal neurons where the power of induced gamma oscillations was decreased by 30%, indicating less network synchronization. This loss of inhibitory tone was hypothesized to lead to hyperexcitability, resulting in loss of synchronization, and this hyperexcitability was observed by evoking action potentials in acute brain slices of variant mice relative to wild type mice, where variant mice exhibited significantly

increased action potential firing frequency relative to wild type, as well as a two-fold higher maximum firing rate per neuron in the variant mouse (Nelson et al., 2020).

To determine the effect of the *ANK3* p.W1989R mutation on GABAergic signaling in mature human-derived neurons, we will perform calcium imaging assays to indicate the activity of neurons in a co-culture. Calcium influx is used as an indicator of neuronal activity, where an influx of calcium indicates action potential firing, and it will be measured using a genetically encoded calcium indicator (GECI), which binds to calcium ions and emits fluorescence to indicate intracellular calcium levels (Fuchs et al., 2013). The resulting activity of neurons in co-culture will be analyzed by software which measures network synchronization through a mean correlation of firing, where a lower mean correlation of firing indicates greater inhibitory input in the network. Here, we will investigate the network synchronization of the bipolar patient-derived neurons relative to controls, as well as a comparison of network synchronization following treatment with bicuculline. Bicuculline is a $GABA_A$ receptor antagonist which prevents the inhibitory current mediated by $GABA_A$ receptors and isolates activity evoked by excitatory input, solely. We hypothesize that prior to bicuculline treatment, the variant-expressing neurons will have lower inhibitory input at baseline, leading to a higher synchronization coefficient, as the activity will be more homogenously influenced by the excitatory activity, relative to the control activity where both excitatory and inhibitory neurons are active. Along this same line of reasoning, we hypothesize that upon bicuculline treatment for both the variant-expressing neurons and controls, the variant will reestablish synchronization more quickly than controls, as the bicuculline isolates excitatory activity only, which was already predominant in the variant neurons. One possible factor that could deviate the obtained results from the hypothesis is that the measured network synchronization by Nelson et al. was measured by gamma oscillations resulting specifically from parvalbumin-positive cortical interneuron activity, and this interneuron subtype cannot yet be fully recapitulated in induced neurons. However, we do expect the differentiation of our inhibitory neurons to results in GABAergic cortical interneuron-like neurons, based on previous results using forced expression of transcription factors ASCL1/DLX2 (Alfred et al., 2016) . Overall, this experiment will allow us to perform comparisons between all genetic backgrounds and establish if the *ANK3* p.W1989R variant is necessary and sufficient to produce decreased GABAergic inhibitory signaling at baseline in co-cultures.

This proposed model and subsequent experimental analyses that will be performed do not come without potential pitfalls, for which alternate strategies can be employed. First, as mentioned, the inability to generate the parvalbumin-positive neuron subtype through the hiPSC-model could result in lack of the hypothesized deficits in GABAergic signaling seen in mixed co-cultures of excitatory and inhibitory hiPSC-derived neurons, relative to those seen in the mouse model (Nelson et al., 2020). However, in the future, the use of novel transcription factors to induce differentiation of hiPSCs could ameliorate this problem, resulting in the generation of parvalbumin-positive-like neurons (Filice et al., 2020). Additionally, it is possible that inhibitory signaling deficits are not observed in the hiPSC-derived neurons, due to the genetic complexity of bipolar disorder, and resulting inability to recapitulate deficits observed in the *ANK3* p.W1989R mouse model. It is possible that observed differences in inhibitory signaling could be due to the technique used, which will be calcium imaging, rather than electrophysiological studies used when observing mouse models (Nelson et al., 2020). In light of this, a fellow lab member who is a specialist in electrophysiology will aid in performing electrophysiological assays as a secondary analysis of functional deficits in the *ANK*3 p.W1989R human-derived model. Finally, based on established role of ankyrin-G in the formation and regulation of the axon initial segment and scaffolding of voltage-gated sodium channels, we could observe alterations in action potential initiation and AIS plasticity in hiPSC derived neurons (Jenkins & Bennett, 2001; Kordeli et al., 1995; Zhou et al., 1998). These deficits in action potential initiation can be detected through electrophysiology, the observed morphology of the AIS, and ion channels scaffolded by ankyrin-G can be studied through immunocytochemistry.

Discussion

The worldwide prevalence of bipolar disorder, as well as its debilitating effects on the patients affected by it, highlight the urgent need to discover the molecular basis of the disease so that more effective treatments can be developed for the disorder. The heritability of the disorder, as well as extensive genome-wide association studies of patients, show that there is a strong genetic basis contributing to its occurrence (Johansson et al., 2019; Song et al., 2015). Further, the discovery of the *ANK3* gene locus, which produces ankyrin-G protein, as one of the most highly associated risk loci provides an important avenue of exploration to discover how *ANK3* variants could contribute to the disease(Ferreira et al., 2008; Sklar et al., 2011; Stahl et al., 2019).

Crucial steps were made by a variety of researchers in discovering that ankyrin-G has a novel role in stabilizing inhibitory (GABAergic) synapses, both *in vitro* and *in vivo,* in the cortical pyramidal and hippocampal neurons of mice (Nelson et al., 2020; Tseng et al., 2015). Further, it was discovered that a critical mutation in the *ANK3* gene, a tryptophan to arginine mutation at position 1989, leads to loss of inhibitory synaptic components, specifically $GABA_A$ receptors through endocytosis, and a functional loss of inhibitory tone in the brains of mice expressing this p.W1989R mutation (Nelson et al., 2020; Tseng et al., 2015). This was seen to be a result of the loss of ankyrin-G association with $GABA_A$ receptor associated protein (GABARAP), a necessary scaffolding intermediate interacting with both $GABA_A$ receptors and ankyrin-G. This disruption in inhibitory signaling is consistent with postmortem brain studies of patients with bipolar disorder where disrupted GABAergic signaling components are repeatedly observed, furthering the connection between *ANK3* variants and bipolar disorder (Benes & Berretta, 2001; Konradi et al., 2011; Torrey et al., 2005). However, these findings in mice are not sufficient to generalize to human patients, as these mice do not recapitulate the disease phenotype and lack the genetic complexity present in human bipolar disorder patients.

Given the present limitations of findings in mouse models, we have begun the work necessary to remedy these challenges using a new model that presents further advantages, using neurons derived from bipolar disorder patients with the *ANK3* p.W1989R variant of interest. As discussed, this model will allow for the generation of functional neuronal populations, both glutamatergic and GABAergic in nature, through forced expression of doxycycline-inducible transcription factors *in vitro* (Alfred et al., 2016; Zhang et al., 2013). These neuronal populations will retain the genetic complexity of the patient including the expression of the variant of interest. Further, the use of hiPSCs allows for generation of genetic controls using CRISPR-mediated genetic reprogramming, so that the variant of interest can be corrected within the patient genetic background, as well as introduced into the genetic background of an age and sex-matched neurotypical control line to assess the necessity and sufficiency of the variant to produce suspected deficits.

The utility of this technique, however, cannot be capitalized upon without sufficient preparatory steps, which I have described throughout this paper. First, the human fibroblasts, gathered from both the patient of interest and an age and sex-matched control individual, had to be reprogrammed using episomal plasmids. This is done to reverse their differentiated state and

induce the characteristics of pluripotent stem cells, including the ability to differentiate into all three germ layers, done by the O'Shea Lab at the University of Michigan. Once these hiPSCs were acquired, for both the BD patient genetic line (BP7G) and the age and sex-matched control patient line (C8WW), it became necessary to maintain these lines in culture over the course of multiple months, to generate a large stock. This came with the trials of optimizing techniques for these cells, such as maintenance, splitting and passing, freezing down, cleaning off excessive spontaneous differentiation, to generate only stem cells with optimal morphology and lack of spontaneous differentiation for storage. Following this, the generation of stable-cell lines with doxycycline-inducible transcription factors for both hiPSC genotypes was done by Kendall Dean and Dr. Michael Uhler over the course of multiple weeks. I repeated the maintenance and freeze-down steps for gathering a large stock of these stable cell lines. Finally, then, could the process of differentiation of hiPSCs to generate neuronal cultures begin, which was halted by widespread mycoplasma contamination. Then we began the process of discovering the causative agent of the mycoplasma contamination, which involved me repeatedly sterilizing all lab equipment, and performing PCR testing on all previous reagents and cell lines. We were eventually able to discover the source of the mycoplasma and discard all contaminated cell lines and reagents. This disrupted all progress towards differentiation and left us with only hiPSCs that had been generated and stored months before. Despite this, I continued past the contamination and completed the process of generating stable cell lines for the hiPSCs of the patient genotype, expressing doxycycline-inducible transcription factors, while Kendall Dean performed the same process using the control genotype hiPSCs.

Future experiments using these hiPSCs to generate mature neuronal cell cultures that maintain the complex genetic background of bipolar disorder patients, as well as control genetic backgrounds, will be used to assess the necessity and sufficiency of the *ANK3* p.W1989R to disrupt inhibitory synapse formation, as well as result in deficits in inhibitory signaling. We expect these future directions to yield results supporting the hypothesis that the *ANK3* p.W1989R mutation, which is found in a cohort of bipolar disorder patients, is necessary and sufficient to cause GABAergic deficits in a human-derived neuron model system.

These experiments, using the patient-derived neurons as opposed to previous experiments using mouse models, will provide key advances to the understanding of the role of ankyrin-G in inhibitory synapse formation in humans, as well as its suspected relationship to bipolar disorder.

First, within the mouse model, the *ANK3* p.W1989R variant is expressed in both pre- and post-synaptic neurons, making it difficult to determine if observed deficits are a result of inhibitory or excitatory neuron deficits. The ability to use co-cultures of excitatory and inhibitory hiPSC-derived neurons with different genetic backgrounds will allow us to isolate the variant to either the pre- or post-synaptic domains, to determine where deficits are observed. Further, the mouse model does not maintain the genetic complexity observed in bipolar disorder patients, making it difficult to extend deficits observed in the mouse model to bipolar patients that express the *ANK3* p.W1989R variant. However, hiPSCs derived from patient fibroblasts maintain the complete genetic background of the patients they are isolated from and allow for the generation of isogenic controls to test the necessity. Further, age- and sex- matched neurotypical control-derived hiPSCs allow for the CRISPR-mediated knock-in of the variant, allowing us to determine sufficiency of the variant to confer deficits. Also, in addition to the *ANK3* p.W1989R variant, GWAS studies have identified an intronic *ANK3* SNP (rs10994318) as a risk allele associated with a 14.5% increase in susceptibility to bipolar disorder (Stahl et al., 2019). Intronic regions have been shown to be capable of influencing gene transcription, and the presence of H3K27 acetylation in this region, often associated with enhancer activity, lead us to predict that this SNP may disrupt a cis regulatory element and decrease the expression of *ANK3* (Shaul, 2017). However, intronic regions are not well conserved across species, making this SNP difficult to characterize in the past. The use of hiPSCs will overcome this mouse model deficit and allow the study of this SNP in an *in-vitro* human-derived model in future experiments. Finally, the use of hiPSCs allows the investigation of how genetic background can influence the response to lithium treatment in bipolar disorder. This is based on findings that only 20-30% of bipolar disorder patients are excellent responders to lithium treatment for mitigating the symptoms of bipolar disorder, and there is very poorly understand variability of lithium efficacy between patients (Papiol et al., 2022). However, GWAS studies have suggested that lithium responsiveness in patients has a genetic basis in a polygenic manner. Further, the mechanism of lithium action at the molecular level is poorly understood (Papiol et al., 2022). However, the use of hiPSCs, that maintain the patient genetic background, will allow for analysis of the cellular response to lithium treatment within lithium-responsive patients, and for connections to be made between specific genotypes and lithium response. Interestingly, the bipolar disorder patient from which our hiPSCs have been derived, expressing the *ANK3* p.W1989R mutation, has a lithium-

responsive phenotype, which will allow for investigation of the cellular results of lithium treatment in hiPSC-derived neurons within this genetic background.

Following the completion of these experiments, further experiments could be done to confirm these results and expand them to apply directly to bipolar disorder. First, electrophysiological analysis by patch clamp, as was done in mouse models, could be utilized in the human-derived neurons in addition to calcium imaging to further assess the functional deficits in GABAergic signaling (Nelson et al., 2020; Tseng et al., 2015). This would provide additional data on the firing characteristics and deficits expected from variant expression. Additionally, it has been observed that lithium, a common treatment for bipolar disorder, can partially restore GABAergic deficits measure in spontaneous inhibitory postsynaptic potential frequency in mouse (Caballero-Florán, unpublished data). This could be applied to hiPSC-derived neurons with bipolar disorder patient genetic background to characterize the effect of lithium in human-derived models. This will provide information on the mechanism of action of one of the pharmaceuticals commonly used to treat bipolar disorder, leading to further development of therapeutics targeting this pathway in the future.

References

Alfred, Yuan, Q., Tan, S., Xiao, Y., Wang, D., Audrey, Sani, L., Tran, H.-D., Kim, P., Yong, Kea, Yen, Y.-C., Huck, Lim, B., & Hyunsoo. (2016). Direct Induction and Functional Maturation of Forebrain GABAergic Neurons from Human Pluripotent Stem Cells. *Cell Reports*, *16*(7), 1942-1953. https://doi.org/10.1016/j.celrep.2016.07.035

Ango, F., di Cristo, G., Higashiyama, H., Bennett, V., Wu, P., & Huang, Z. J. (2004). Ankyrin-Based Subcellular Gradient of Neurofascin, an Immunoglobulin Family Protein, Directs GABAergic Innervation at Purkinje Axon Initial Segment. *Cell*, *119*(2), 257-272. https://doi.org/10.1016/j.cell.2004.10.004

Beers, J., Gulbranson, D. R., George, N., Siniscalchi, L. I., Jones, J., Thomson, J. A., & Chen, G. (2012). Passaging and colony expansion of human pluripotent stem cells by enzyme-free dissociation in chemically defined culture conditions. *Nat Protoc*, *7*(11), 2029-2040. https://doi.org/10.1038/nprot.2012.130

Benes, F. M., & Berretta, S. (2001). GABAergic Interneurons: Implications for Understanding Schizophrenia and Bipolar Disorder. *Neuropsychopharmacology*, *25*(1), 1-27. https://doi.org/10.1016/S0893-133X(01)00225-1

Bennett, V. (1979). Immunoreactive forms of human erythrocyte ankyrin are present in diverse cells and tissues. *Nature*, *281*(5732), 597-599. https://doi.org/10.1038/281597a0

Bennett, V., & Lorenzo, D. N. (2013). Chapter One - Spectrin- and Ankyrin-Based Membrane Domains and the Evolution of Vertebrates. In V. Bennett (Ed.), *Current Topics in Membranes* (Vol. 72, pp. 1-37). Academic Press. https://doi.org/https://doi.org/10.1016/B978-0-12-417027-8.00001-5

Birgisdottir Å, B., Lamark, T., & Johansen, T. (2013). The LIR motif - crucial for selective autophagy. *J Cell Sci*, *126*(Pt 15), 3237-3247. https://doi.org/10.1242/jcs.126128

Bressler, S. L., & Menon, V. (2010). Large-scale brain networks in cognition: emerging methods and principles. *Trends Cogn Sci*, *14*(6), 277-290. https://doi.org/10.1016/j.tics.2010.04.004

Chang, K.-J., & Rasband, M. N. (2013). Chapter Five - Excitable Domains of Myelinated Nerves: Axon Initial Segments and Nodes of Ranvier. In V. Bennett (Ed.), *Current Topics in Membranes* (Vol. 72, pp. 159-192). Academic Press. https://doi.org/https://doi.org/10.1016/B978-0-12-417027-8.00005-2

Collins, A. L., & Sullivan, P. F. (2013). Genome-wide association studies in psychiatry: what have we learned? *Br J Psychiatry*, *202*(1), 1-4. https://doi.org/10.1192/bjp.bp.112.117002

Corvin, A., Craddock, N., & Sullivan, P. F. (2010). Genome-wide association studies: a primer. *Psychol Med*, *40*(7), 1063-1077. https://doi.org/10.1017/s0033291709991723

Craddock, N., & Jones, I. (1999). Genetics of bipolar disorder. *J Med Genet*, *36*(8), 585-594. https://doi.org/10.1136/jmg.36.8.585

Cunha, S. R., & Mohler, P. J. (2009). Ankyrin protein networks in membrane formation and stabilization. *Journal of Cellular and Molecular Medicine*, *13*(11-12), 4364-4376. https://doi.org/https://doi.org/10.1111/j.1582-4934.2009.00943.x

Das, A. T., Tenenbaum, L., & Berkhout, B. (2016). Tet-On Systems For Doxycycline-inducible Gene Expression. *Curr Gene Ther*, *16*(3), 156-167. https://doi.org/10.2174/1566523216666160524144041

Dols, A., Sienaert, P., van Gerven, H., Schouws, S., Stevens, A., Kupka, R., & Stek, M. L. (2013). The prevalence and management of side effects of lithium and anticonvulsants as mood stabilizers in bipolar disorder from a clinical perspective: a review. *International Clinical Psychopharmacology*, *28*(6). https://journals.lww.com/intclinpsychopharm/Fulltext/2013/11000/The_prevalence_and_management_of_side_effects_of.1.aspx

Dome, P., Rihmer, Z., & Gonda, X. (2019). Suicide Risk in Bipolar Disorder: A Brief Review. *Medicina (Kaunas)*, *55*(8). https://doi.org/10.3390/medicina55080403

Dzhashiashvili , Y., Zhang , Y., Galinska , J., Lam , I., Grumet , M., & Salzer , J. L. (2007). Nodes of Ranvier and axon initial segments are ankyrin G–dependent domains that assemble by distinct mechanisms. *Journal of Cell Biology*, *177*(5), 857-870. https://doi.org/10.1083/jcb.200612012

Ferreira, M. A. R., O'Donovan, M. C., Meng, Y. A., Jones, I. R., Ruderfer, D. M., Jones, L., Fan, J., Kirov, G., Perlis, R. H., Green, E. K., Smoller, J. W., Grozeva, D., Stone, J., Nikolov, I., Chambert, K., Hamshere, M. L., Nimgaonkar, V. L., Moskvina, V., Thase, M. E., . . . Wellcome Trust Case Control, C. (2008). Collaborative genome-wide association analysis supports a role for ANK3 and CACNA1C in bipolar disorder. *Nature Genetics*, *40*(9), 1056-1058. https://doi.org/10.1038/ng.209

Filice, F., Schwaller, B., Michel, T. M., & Grünblatt, E. (2020). Profiling parvalbumin interneurons using iPSC: challenges and perspectives for Autism Spectrum Disorder (ASD). *Mol Autism*, *11*(1), 10. https://doi.org/10.1186/s13229-020-0314-0

Fiorentino, A., O'Brien, N. L., Locke, D. P., McQuillin, A., Jarram, A., Anjorin, A., Kandaswamy, R., Curtis, D., Blizard, R. A., & Gurling, H. M. D. (2014). Analysis of ANK3 and CACNA1C variants identified in bipolar disorder whole genome sequence data [https://doi.org/10.1111/bdi.12203]. *Bipolar Disorders*, *16*(6), 583-591. https://doi.org/https://doi.org/10.1111/bdi.12203

Fuchs, C., Abitbol, K., Burden, J. J., Mercer, A., Brown, L., Iball, J., Anne Stephenson, F., Thomson, A. M., & Jovanovic, J. N. (2013). GABA(A) receptors can initiate the formation of functional inhibitory GABAergic synapses. *Eur J Neurosci*, *38*(8), 3146-3158. https://doi.org/10.1111/ejn.12331

Geddes, J. R., & Miklowitz, D. J. (2013). Treatment of bipolar disorder. *The Lancet*, *381*(9878), 1672-1682. https://doi.org/https://doi.org/10.1016/S0140-6736(13)60857-0

Genomewide Association Studies: History, Rationale, and Prospects for Psychiatric Disorders. (2009). *American Journal of Psychiatry*, *166*(5), 540-556. https://doi.org/10.1176/appi.ajp.2008.08091354

Grande, I., Berk, M., Birmaher, B., & Vieta, E. (2016). Bipolar disorder. *The Lancet*, *387*(10027), 1561-1572. https://doi.org/https://doi.org/10.1016/S0140-6736(15)00241-X

Gupta, S., M-Redmond, T., Meng, F., Tidball, A., Akil, H., Watson, S., Parent, J. M., & Uhler, M. (2018). Fibroblast growth factor 2 regulates activity and gene expression of human post-mitotic excitatory neurons [https://doi.org/10.1111/jnc.14255]. *Journal of Neurochemistry*, *145*(3), 188-203. https://doi.org/https://doi.org/10.1111/jnc.14255

Harrison, P. J. (2016). Molecular neurobiological clues to the pathogenesis of bipolar disorder. *Current Opinion in Neurobiology*, *36*, 1-6. https://doi.org/https://doi.org/10.1016/j.conb.2015.07.002

Hay, R. J., Macy, M. L., & Chen, T. R. (1989). Mycoplasma infection of cultured cells. *Nature*, *339*(6224), 487-488. https://doi.org/10.1038/339487a0

Hedstrom, K. L., Ogawa, Y., & Rasband, M. N. (2008). AnkyrinG is required for maintenance of the axon initial segment and neuronal polarity. *J Cell Biol*, *183*(4), 635-640. https://doi.org/10.1083/jcb.200806112

Hedstrom, K. L., & Rasband, M. N. (2006). Intrinsic and extrinsic determinants of ion channel localization in neurons. *Journal of Neurochemistry*, *98*(5), 1345-1352. https://doi.org/https://doi.org/10.1111/j.1471-4159.2006.04001.x

Hoock, T. C., Peters, L. L., & Lux, S. E. (1997). Isoforms of Ankyrin-3 That Lack the NH2-terminal Repeats Associate with Mouse Macrophage Lysosomes. *Journal of Cell Biology*, *136*(5), 1059-1070. https://doi.org/10.1083/jcb.136.5.1059

Howe, J. R., Bear, M. F., Golshani, P., Klann, E., Lipton, S. A., Mucke, L., Sahin, M., & Silva, A. J. (2018). The mouse as a model for neuropsychiatric drug development. *Current Biology*, *28*(17), R909-R914. https://doi.org/https://doi.org/10.1016/j.cub.2018.07.046

Jenkins, P. M., Kim, N., Jones, S. L., Tseng, W. C., Svitkina, T. M., Yin, H. H., & Bennett, V. (2015). Giant ankyrin-G: A critical innovation in vertebrate evolution of fast and integrated neuronal signaling. *Proceedings of the National Academy of Sciences*, *112*(4), 957-964. https://doi.org/doi:10.1073/pnas.1416544112

Jenkins, S. M., & Bennett, V. (2001). Ankyrin-G coordinates assembly of the spectrin-based membrane skeleton, voltage-gated sodium channels, and L1 CAMs at Purkinje neuron initial segments. *J Cell Biol*, *155*(5), 739-746. https://doi.org/10.1083/jcb.200109026

Johansson, V., Kuja-Halkola, R., Cannon, T. D., Hultman, C. M., & Hedman, A. M. (2019). A population-based heritability estimate of bipolar disorder - In a Swedish twin sample. *Psychiatry Res*, *278*, 180-187. https://doi.org/10.1016/j.psychres.2019.06.010

Kerner, B. (2014). Genetics of bipolar disorder. *Appl Clin Genet*, *7*, 33-42. https://doi.org/10.2147/tacg.S39297

Kittler, J. T., Delmas, P., Jovanovic, J. N., Brown, D. A., Smart, T. G., & Moss, S. J. (2000). Constitutive endocytosis of GABAA receptors by an association with the adaptin AP2 complex modulates inhibitory synaptic currents in hippocampal neurons. *J Neurosci*, *20*(21), 7972-7977. https://doi.org/10.1523/jneurosci.20-21-07972.2000

Konradi, C., Zimmerman, E. I., Yang, C. K., Lohmann, K. M., Gresch, P., Pantazopoulos, H., Berretta, S., & Heckers, S. (2011). Hippocampal interneurons in bipolar disorder. *Arch Gen Psychiatry*, *68*(4), 340-350. https://doi.org/10.1001/archgenpsychiatry.2010.175

Kordeli, E., Lambert, S., & Bennett, V. (1995). Ankyrin: A NEW ANKYRIN GENE WITH NEURAL-SPECIFIC ISOFORMS LOCALIZED AT THE AXONAL INITIAL

SEGMENT AND NODE OF RANVIER (∗). *Journal of Biological Chemistry*, *270*(5), 2352-2359. https://doi.org/10.1074/jbc.270.5.2352

Kulessa, H., Frampton, J., & Graf, T. (1995). GATA-1 reprograms avian myelomonocytic cell lines into eosinophils, thromboblasts, and erythroblasts. *Genes Dev*, *9*(10), 1250-1262. https://doi.org/10.1101/gad.9.10.1250

Kunimoto, M., Otto, E., & Bennett, V. (1991). A new 440-kD isoform is the major ankyrin in neonatal rat brain. *J Cell Biol*, *115*(5), 1319-1331. https://doi.org/10.1083/jcb.115.5.1319

Lambert, S., & Bennett, V. (1993). Postmitotic expression of ankyrinR and beta R-spectrin in discrete neuronal populations of the rat brain. *J Neurosci*, *13*(9), 3725-3735. https://doi.org/10.1523/jneurosci.13-09-03725.1993

Leterrier, C., Vacher, H., Fache, M. P., d'Ortoli, S. A., Castets, F., Autillo-Touati, A., & Dargent, B. (2011). End-binding proteins EB3 and EB1 link microtubules to ankyrin G in the axon initial segment. *Proc Natl Acad Sci U S A*, *108*(21), 8826-8831. https://doi.org/10.1073/pnas.1018671108

Luscher, B., Fuchs, T., & Kilpatrick, C. L. (2011). GABAA receptor trafficking-mediated plasticity of inhibitory synapses. *Neuron*, *70*(3), 385-409. https://doi.org/10.1016/j.neuron.2011.03.024

Machado-Vieira, R., Kapczinski, F., & Soares, J. C. (2004). Perspectives for the development of animal models of bipolar disorder. *Progress in Neuro-Psychopharmacology and Biological Psychiatry*, *28*(2), 209-224. https://doi.org/https://doi.org/10.1016/j.pnpbp.2003.10.015

Marín, O. (2012). Interneuron dysfunction in psychiatric disorders. *Nature Reviews Neuroscience*, *13*(2), 107-120. https://doi.org/10.1038/nrn3155

Markoullis, K., Bulian, D., Hölzlwimmer, G., Quintanilla-Martinez, L., Heiliger, K. J., Zitzelsberger, H., Scherb, H., Mysliwietz, J., Uphoff, C. C., Drexler, H. G., Adler, T., Busch, D. H., Schmidt, J., & Mahabir, E. (2009). Mycoplasma contamination of murine embryonic stem cells affects cell parameters, germline transmission and chimeric progeny. *Transgenic Res*, *18*(1), 71-87. https://doi.org/10.1007/s11248-008-9218-z

McElroy, S. L., Altshuler, L. L., Suppes, T., Keck, P. E., Frye, M. A., Denicoff, K. D., Nolen, W. A., Kupka, R. W., Leverich, G. S., Rochussen, J. R., Rush, A. J., & Post, R. M. (2001). Axis I Psychiatric Comorbidity and Its Relationship to Historical Illness

Variables in 288 Patients With Bipolar Disorder. *American Journal of Psychiatry*, *158*(3), 420-426. https://doi.org/10.1176/appi.ajp.158.3.420

Merikangas, K. R., Jin, R., He, J.-P., Kessler, R. C., Lee, S., Sampson, N. A., Viana, M. C., Andrade, L. H., Hu, C., Karam, E. G., Ladea, M., Medina-Mora, M. E., Ono, Y., Posada-Villa, J., Sagar, R., Wells, J. E., & Zarkov, Z. (2011). Prevalence and Correlates of Bipolar Spectrum Disorder in the World Mental Health Survey Initiative. *Archives of General Psychiatry*, *68*(3), 241. https://doi.org/10.1001/archgenpsychiatry.2011.12

Mullins, N., Forstner, A. J., O'Connell, K. S., Coombes, B., Coleman, J. R. I., Qiao, Z., Als, T. D., Bigdeli, T. B., Børte, S., Bryois, J., Charney, A. W., Drange, O. K., Gandal, M. J., Hagenaars, S. P., Ikeda, M., Kamitaki, N., Kim, M., Krebs, K., Panagiotaropoulou, G., . . . Andreassen, O. A. (2021). Genome-wide association study of more than 40,000 bipolar disorder cases provides new insights into the underlying biology. *Nature Genetics*, *53*(6), 817-829. https://doi.org/10.1038/s41588-021-00857-4

Nelson, A. D., Caballero-Florán, R. N., Rodríguez Díaz, J. C., Hull, J. M., Yuan, Y., Li, J., Chen, K., Walder, K. K., Lopez-Santiago, L. F., Bennett, V., McInnis, M. G., Isom, L. L., Wang, C., Zhang, M., Jones, K. S., & Jenkins, P. M. (2020). Ankyrin-G regulates forebrain connectivity and network synchronization via interaction with GABARAP. *Molecular Psychiatry*, *25*(11), 2800-2817. https://doi.org/10.1038/s41380-018-0308-x

Nelson, A. D., & Jenkins, P. M. (2016). The Splice Is Right: ANK3 and the Control of Cortical Circuits. *Biol Psychiatry*, *80*(4), 263-265. https://doi.org/10.1016/j.biopsych.2016.06.006

Nestler, E. J., & Hyman, S. E. (2010). Animal models of neuropsychiatric disorders. *Nature Neuroscience*, *13*(10), 1161-1169. https://doi.org/10.1038/nn.2647

Nikfarjam, L., & Farzaneh, P. (2012). Prevention and detection of Mycoplasma contamination in cell culture. *Cell J*, *13*(4), 203-212.

Okita, K., Matsumura, Y., Sato, Y., Okada, A., Morizane, A., Okamoto, S., Hong, H., Nakagawa, M., Tanabe, K., Tezuka, K.-i., Shibata, T., Kunisada, T., Takahashi, M., Takahashi, J., Saji, H., & Yamanaka, S. (2011). A more efficient method to generate integration-free human iPS cells. *Nature Methods*, *8*(5), 409-412. https://doi.org/10.1038/nmeth.1591

Otto, E., Kunimoto, M., McLaughlin, T., & Bennett, V. (1991). Isolation and characterization of cDNAs encoding human brain ankyrins reveal a family of alternatively spliced genes. *J Cell Biol*, *114*(2), 241-253. https://doi.org/10.1083/jcb.114.2.241

Papiol, S., Schulze, T. G., & Heilbronner, U. (2022). Lithium response in bipolar disorder: Genetics, genomics, and beyond. *Neuroscience Letters*, *785*, 136786. https://doi.org/https://doi.org/10.1016/j.neulet.2022.136786

Rottem, S., & Barile, M. F. (1993). Beware of mycoplasmas. *Trends in Biotechnology*, *11*(4), 143-151. https://doi.org/https://doi.org/10.1016/0167-7799(93)90089-R

Schulze, T. G., Detera-Wadleigh, S. D., Akula, N., Gupta, A., Kassem, L., Steele, J., Pearl, J., Strohmaier, J., Breuer, R., Schwarz, M., Propping, P., Nöthen, M. M., Cichon, S., Schumacher, J., Rietschel, M., McMahon, F. J., & Consortium, N. G. I. B. D. (2009). Two variants in Ankyrin 3 (ANK3) are independent genetic risk factors for bipolar disorder. *Molecular Psychiatry*, *14*(5), 487-491. https://doi.org/10.1038/mp.2008.134

Shaul, O. (2017). How introns enhance gene expression. *Int J Biochem Cell Biol*, *91*(Pt B), 145-155. https://doi.org/10.1016/j.biocel.2017.06.016

Shinozaki, G., & Potash, J. B. (2014). New Developments in the Genetics of Bipolar Disorder. *Current Psychiatry Reports*, *16*(11), 493. https://doi.org/10.1007/s11920-014-0493-5

Sklar, P., Ripke, S., Scott, L. J., Andreassen, O. A., Cichon, S., Craddock, N., Edenberg, H. J., Nurnberger, J. I., Rietschel, M., Blackwood, D., Corvin, A., Flickinger, M., Guan, W., Mattingsdal, M., McQuillin, A., Kwan, P., Wienker, T. F., Daly, M., Dudbridge, F., . . . Psychiatric, G. C. B. D. W. G. (2011). Large-scale genome-wide association analysis of bipolar disorder identifies a new susceptibility locus near ODZ4. *Nature Genetics*, *43*(10), 977-983. https://doi.org/10.1038/ng.943

Solomon, D. A., Keitner, G. I., Miller, I. W., Shea, M. T., & Keller, M. B. (1995). Course of illness and maintenance treatments for patients with bipolar disorder. *J Clin Psychiatry*, *56*(1), 5-13.

Song, J., Bergen, S. E., Kuja-Halkola, R., Larsson, H., Landén, M., & Lichtenstein, P. (2015). Bipolar disorder and its relation to major psychiatric disorders: a family-based study in the Swedish population. *Bipolar Disord*, *17*(2), 184-193. https://doi.org/10.1111/bdi.12242

Stahl, E. A., Breen, G., Forstner, A. J., McQuillin, A., Ripke, S., Trubetskoy, V., Mattheisen, M., Wang, Y., Coleman, J. R. I., Gaspar, H. A., De Leeuw, C. A., Steinberg, S., Pavlides, J. M. W., Trzaskowski, M., Byrne, E. M., Pers, T. H., Holmans, P. A., Richards, A. L., Abbott, L., . . . Sklar, P. (2019). Genome-wide association study identifies 30 loci associated with bipolar disorder. *Nature Genetics*, *51*(5), 793-803. https://doi.org/10.1038/s41588-019-0397-8

Tada, M., Takahama, Y., Abe, K., Nakatsuji, N., & Tada, T. (2001). Nuclear reprogramming of somatic cells by in vitro hybridization with ES cells. *Current Biology*, *11*(19), 1553-1558. https://doi.org/10.1016/S0960-9822(01)00459-6

Tak, Y. G., & Farnham, P. J. (2015). Making sense of GWAS: using epigenomics and genome engineering to understand the functional relevance of SNPs in non-coding regions of the human genome. *Epigenetics & Chromatin*, *8*(1), 57. https://doi.org/10.1186/s13072-015-0050-4

Takahashi, K., & Yamanaka, S. (2016). A decade of transcription factor-mediated reprogramming to pluripotency. *Nature Reviews Molecular Cell Biology*, *17*(3), 183-193. https://doi.org/10.1038/nrm.2016.8

Torrey, E. F., Barci, B. M., Webster, M. J., Bartko, J. J., Meador-Woodruff, J. H., & Knable, M. B. (2005). Neurochemical markers for schizophrenia, bipolar disorder, and major depression in postmortem brains. *Biological Psychiatry*, *57*(3), 252-260. https://doi.org/https://doi.org/10.1016/j.biopsych.2004.10.019

Tremblay, R., Lee, S., & Rudy, B. (2016). GABAergic Interneurons in the Neocortex: From Cellular Properties to Circuits. *Neuron*, *91*(2), 260-292. https://doi.org/https://doi.org/10.1016/j.neuron.2016.06.033

Tseng, W. C., Jenkins, P. M., Tanaka, M., Mooney, R., & Bennett, V. (2015). Giant ankyrin-G stabilizes somatodendritic GABAergic synapses through opposing endocytosis of GABA _A receptors. *Proceedings of the National Academy of Sciences*, *112*(4), 1214-1219. https://doi.org/10.1073/pnas.1417989112

Unsain, N., Stefani, F. D., & Cáceres, A. (2018). The Actin/Spectrin Membrane-Associated Periodic Skeleton in Neurons [Mini Review]. *Frontiers in Synaptic Neuroscience*, *10*. https://doi.org/10.3389/fnsyn.2018.00010

Wang, C., Ward, M. E., Chen, R., Liu, K., Tracy, T. E., Chen, X., Xie, M., Sohn, P. D., Ludwig, C., Meyer-Franke, A., Karch, C. M., Ding, S., & Gan, L. (2017). Scalable Production of iPSC-Derived Human Neurons to Identify Tau-Lowering Compounds by High-Content Screening. *Stem Cell Reports*, *9*(4), 1221-1233. https://doi.org/10.1016/j.stemcr.2017.08.019

Xie, H., Ye, M., Feng, R., & Graf, T. (2004). Stepwise Reprogramming of B Cells into Macrophages. *Cell*, *117*(5), 663-676. https://doi.org/10.1016/S0092-8674(04)00419-2

Yang, N., Chanda, S., Marro, S., Ng, Y. H., Janas, J. A., Haag, D., Ang, C. E., Tang, Y., Flores, Q., Mall, M., Wapinski, O., Li, M., Ahlenius, H., Rubenstein, J. L., Chang, H. Y., Buylla, A. A., Südhof, T. C., & Wernig, M. (2017). Generation of pure GABAergic neurons by transcription factor programming. *Nat Methods*, *14*(6), 621-628. https://doi.org/10.1038/nmeth.4291

Zhang, Y., Pak, C., Han, Y., Ahlenius, H., Zhang, Z., Chanda, S., Marro, S., Patzke, C., Acuna, C., Covy, J., Xu, W., Yang, N., Danko, T., Chen, L., Wernig, M., & Thomas. (2013). Rapid Single-Step Induction of Functional Neurons from Human Pluripotent Stem Cells. *Neuron*, *78*(5), 785-798. https://doi.org/10.1016/j.neuron.2013.05.029

Zhao, S., Jiang, E., Chen, S., Gu, Y., Shangguan, A. J., Lv, T., Luo, L., & Yu, Z. (2016). PiggyBac transposon vectors: the tools of the human gene encoding. *Transl Lung Cancer Res*, *5*(1), 120-125. https://doi.org/10.3978/j.issn.2218-6751.2016.01.05

Zhou, D., Lambert, S., Malen, P. L., Carpenter, S., Boland, L. M., & Bennett, V. (1998). AnkyrinG Is Required for Clustering of Voltage-gated Na Channels at Axon Initial Segments and for Normal Action Potential Firing. *Journal of Cell Biology*, *143*(5), 1295-1304. https://doi.org/10.1083/jcb.143.5.1295